THE TRANSITION FROM TWO PHASE BUBBLE FLOW TO SLUG FLOW

NICK A. RADOVCICH
RAPHAEL MOISSIS

June 1962

Report No. 7-7673-22
Department of Mechanical Engineering
Massachusetts Institute of Technology

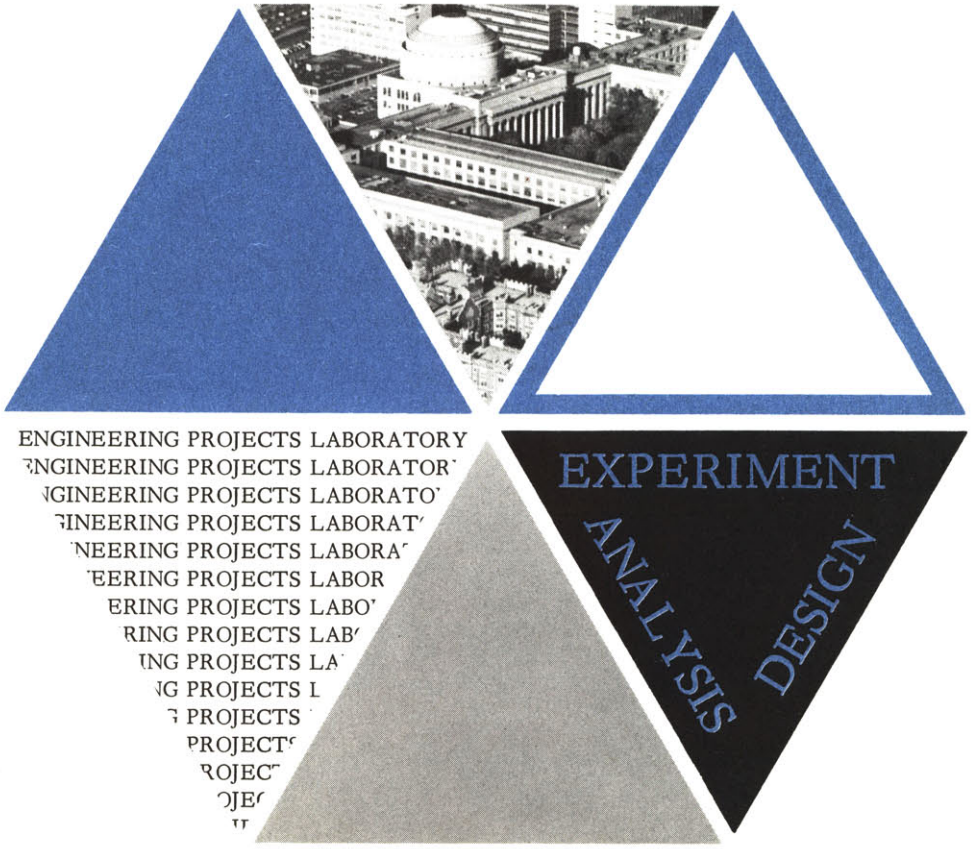

TECHNICAL REPORT NO. 22

THE TRANSITION FROM TWO PHASE BUBBLE FLOW TO SLUG FLOW

by

Nick A. Radovcich*
and
Raphael Moissis**

For

THE OFFICE OF NAVAL RESEARCH

NONR - 1841 (39)

DSR No. 7-7673

June 1962

Division of Sponsored Research
Massachusetts Institute of Technology
Cambridge 39, Massachusetts

* Research Assistant, Department of Mechanical Engineering, M.I.T.

** Assistant Professor of Mechanical Engineering, M.I.T.

ABSTRACT

The process of transition from bubble to slug flow in a vertical pipe has been studied analytically and experimentally.

An equation is presented which gives the agglomeration time as a function of void fraction, channel diameter, initial bubble diameter and liquid purity. A dependent function which also appears in the equation has been evaluated using experimental data.

A reasonably good correlation of the data has been achieved.

ACKNOWLEDGEMENTS

This work has been entirely supported by the Office of Naval Research and has been performed in the Heat Transfer Laboratory of the Massachusetts Institute of Technology, which is under the direction of Professor W. M. Rohsenow.

We wish to express our thanks to Professor P. Griffith for his many helpful suggestions and criticisms.

TABLE OF CONTENTS

1. INTRODUCTION

When two phases flow together in a tube they can distribute themselves in a number of different configurations. The flow configuration assumed by a two phase mixture depends on certain parameters such as volume flow rates of the two phases, flow direction of each component, channel orientation, distance from pipe inlet, fluid properties and heat transfer conditions.

Figure 1 illustrates the flow configurations that may exist when a gas and a liquid flow concurrently upwards in a vertical tube.

Bubble flow is characterized by bubbles which are small compared to the tube diameter. These bubbles, which are dispersed randomly within the tube, rise with different velocities depending on the bubble size.

Slug flow is characterized by large bubbles (G. I. Taylor bubbles) separated by slugs of liquid. One may or may not find small bubbles in the slug following the Taylor bubble. When the separation distance between two Taylor bubbles is large, all bubbles rise with a uniform velocity. This type of flow is termed fully developed slug flow. On the other hand, when the separation distance between two Taylor bubbles is smaller than some critical value, each bubble is influenced by the wake of the bubble ahead of it. Bubbles continually agglomerate with one another, break up into small bubbles and agglomerate again. This type of flow is termed developing slug flow (1)*, or semi-annular flow (2).

Annular flow exists when the liquid flows in an annulus around a core which is occupied by the gas.

---

* Numbers in parentheses refer to a similarly numbered bibliography at the end of this work.

Finally, mist flow is a high velocity gas stream with minute liquid drops entrained in it.

Experimental observations have shown that fully developed slug flow, annular flow and mist flow are stable flow configurations. These can, therefore, be defined as stable flow regimes as opposed to unstable configurations which will be termed transient flow regimes.

Bubble flow, which is of primary importance in this study, has shown a distinct reluctance to retaining its identity in very long pipes. It is, therefore, suggested that bubble flow is a transient flow regime. Given a sufficiently long residence time in a pipe, a swarm of bubbles will ultimately be reduced to a stable slug flow.

Since, however, under certain conditions, the transition from bubble to slug flow requires a long period of time, bubble flow through a tube of finite length may appear as a stable configuration. In such a case pressure drop, heat transfer or stability calculations may be based on some bubble flow model (e.g. (3), (4)). On the other hand, in an adiabatic and (much more so) a non-adiabatic system of sufficient length, bubble flow may exist up to a certain height whereas the flow pattern above that height changes to a developing or a fully developed slug flow.

The present investigation is concerned with answering the question: "When does a given bubble flow system become slug flow in character?" The work reported here is, in other words, an investigation of the bubble to slug transition process.

2.0 PARAMETERS GOVERNING BUBBLE TO SLUG TRANSITION

2.1 The Agglomeration Point

As work progressed, it became necessary to define clearly the first flow pattern which would be termed slug flow. The terms "agglomeration point" and "first identifiable existence of slug flow," as used in this report, are synonymous and define a point in the flow field where a G. I. Taylor bubble or an effective G. I. Taylor bubble first appears and retains its identity.

By definition, a Taylor bubble is a constant pressure surface whose shape is that of a cylinder bounded on top by a spherical cap or a bullet shaped nose, and at the bottom by a distorted flat tail. The mean diameter of the bubble cylinder is almost equal to the tube diameter. To be distinguished from a spherical cap, the length of a Taylor bubble is at least one tube diameter.

Suppose that a swarm of small bubbles packed themselves into a shape similar to that of a Taylor bubble. As outside bubble layers coalesce, they enclose the remaining bubbles in a nearly constant pressure envelope, thus making the swarm appear more and more like a Taylor bubble. This bullet-shaped swarm of bubbles may be considered as an effective Taylor bubble, because the velocity profile behind it, the pressure recorded by a pressure tap at its sides, the oscillatory nature of the flow etc., are all the same as if the swarm was indeed a single bubble.

Since in essence an agglomeration point indicates where bubble flow ceases to exist, no distinction need be made between an actual and an effective Taylor bubble. The appearance of either an actual or an effective Taylor bubble which retains its identity defines the transition to slug flow.

2.2 Important Liquid and Gas Properties

2.2.1 Normal Fluid Properties

The static surface tension*, the viscosities and densities of the two phases are important parameters in governing the bubble-slug transition process. These properties affect the bubble rise velocities, the mixing action between bubbles etc. While these properties are easily defined and controlled experimentally, they in themselves do not suffice to define completely the liquid-gas state. There exists some other fluid property which when varied changes the flow field significantly.

2.2.2 Special Fluid Properties

a. Purity

Freedom from foreign matter in a liquid is generally referred to as purity. Two types of impurities may be distinguished. First, foreign matter that dissolves homogeneously in the liquid, and second matter that retains its macroscopic identity being merely suspended in the fluid. The former will be referred to as chemical purity and the latter as particle purity.

A few preliminary experiments established that purity is an extremely difficult quantity to define. However, without definition, control, and quantitative analysis of purity, experimental results can, at best, only

* The term "static surface tension" is used here to distinguish it from "dynamic surface tension." A definition of the two is given in section 2.2.2.

indicate trends. Thus, a major effort was initiated in this area. Detailed discussion of this effort is given in a later section.

b. Dynamic Surface Tension

When at rest for a long period of time, the interface between two fluids behaves as if it were in a state of uniform tension. The interface can be represented mathematically as a geometric surface in tension. This representation, which is the basis of the treatment of capillarity in classical hydrodynamics, defines the property (static) surface tension. In contrast with the role of (static) surface tension, the part played in free-boundary flows by other interfacial properties is not well understood. Of particular importance to the present study are the properties pertaining to the resistance of an interface to deformation.

A literature survey into the dynamics of films, stability of foams, and drop and bubble motions reveals that there are two quantities which are believed to be important in interfacial dynamics. Although these quantities appear to be different from one another, both are referred to in the literature as dynamic surface tensions. A clear description and differentiation of these two properties will be attempted.

The first quantity is used to describe the surface free energy of a newly formed surface. The "dynamic" surface tension measurement is made on a surface within a small fraction of a second after the formation (extension) of the surface, before there has been time for the normal difference in concentration between surface layer and bulk of the solution to establish itself. In this sense, "dynamic surface tension" does not define a new property but simply a temporary value of the property "static surface tension."

Measurements of the dynamic surface tension are made by determining the distance between the nodal points on a stream flowing from an elongated orifice. Since such a stream is moving at a rapid rate, and since its surface dates from its emergence from the orifice, the measurements are made within a small fraction of a second after the formation of the surface.

The amount of time needed for a surface to attain its normal (static) free energy depends largely on the type of solution (5). It may take seconds, minutes, or even several hours. In extremely dilute solutions it is reported by several investigators (5) that the attainment of the final surface tension takes several days. Finally, in the case of some soaps, the change in surface free energy may continue

indefinitely probably because of hydrolysis of the soap. In addition to the dynamic surface tension just described (due to "ageing",) classical hydrodynamics also recognizes that extension and contraction of a surface film produce dynamic variations of surface tension, which in turn give rise to discontinuities in the tangential components of fluid stress at the interface. To distinguish this effect from that of "ageing," it will be convenient to refer to that surface property which is due to surface dilatational elasticity or viscosity as the "second coefficient of surface tension."

It should be noted that according to the description given above, in pure liquids static and dynamic surface tensions become identical (because there is no difference in concentration between surface and bulk) whereas the second coefficient of surface tension is a separate quantity which - according to theory - comes into play when a surface is deformed even in a pure liquid.

The importance of the second coefficient of surface tension to the stability of a bubble has been emphasized by several authors (6, 7, 8, 9). Since, however, no satisfactory method is known for its measurement, quantitative confirmation of its existence is lacking.

Evidence reported in this paper and elsewhere (10) suggests that the non-uniform tension effects, and

in turn the ability of an interface to resist deformation, are sensitive to purity of the system.

2.3 Volume Quality and Froude Number

The parameters volume quality $\Phi = \frac{Q_g}{Q_f + Q_g}$

and Froude number $N_{FR} = \left(\frac{Q_f + Q_g}{A_p}\right)^2 / g D_p$

which were originally proposed by Kozlov (7) appear to be the most appropriate co-ordinates in a two phase flow regime map. A recently proposed map (12) is shown in Figure 2. It is seen that the transition lines shown in earlier maps have been replaced by fairly wide bands. The reason for this uncertainty is that volume quality and Froude number alone are not sufficient to describe a transition process. Thus, the transition from slug flow to froth or fog flow has been described analytically (13) and shown to depend on tube diameter and Weber number in addition to the Kozlov parameters. Since bubble flow is not a stable flow regime, another parameter must be introduced in the bubble to slug transition band, namely the length of pipe considered. As mentioned earlier in this report, a flow with specified properties, purity, Φ and N_{FR} may appear as a bubble flow for the first 10, 20, or even several hundred diameters length, but exhibit slug flow characteristics beyond that.

3.0 ANALYTICAL CONSIDERATIONS

Because of the complicated geometry and interfacial boundary conditions involved, a direct mathematical approach to the bubble-slug transition, starting from the general equations of fluid mechanics is not possible at present. The closest situations to the present problem which have been considered in the literature are the interactions of two bubbles in potential flow (14), and the interactions of two or more bubbles in Stokes' flow (15, 16). The assumptions in either of these types of solutions are such that they cannot be applied in a useful way to the problem at hand. Moreover, a description of the motion of a swarm of bubbles which is prescribed in (17) cannot be applied to the present problem because in that experiment, the bubble diameter was much larger than the separation distance between the bubbles.

In light of the problem complexity, a model was sought which would be both simple enough to be workable as well as accurate enough to represent the actual phenomenon involved.

In the early stages of this work, attempts were made to define a control volume model which might describe or help correlate the observed phenomena without examining the dynamics or stability of the individual bubbles. The strong influence of water purity on the agglomeration process revealed that the process could not be described or completely understood without studies of the stability of bubbles and the films that separate them. This conclusion leads eventually to the consideration of the "bubble collision" model.

Since it has been possible to derive from this model definitive equations which agree with data, it is believed, at the time of writing, that the collision model gives a basically correct description of this complicated phenomenon. More data and more particularly, a better understanding of interfacial dynamics is needed before this model can give more general results. The two models considered, the "control volume" and the "bubble collision" model, will be described briefly in the following two sections.

3.1 The Control Volume Model

The idealized control volume model is shown in Figure 3. A swarm of bubbles initially contained in a cylindrical semi-permeable membrane (which allows only liquid to flow through it) is assumed to be compressed to the final shape of a Taylor bubble by a distributed external force F. This force is assumed to be independent of the bubble size and distribution, and dependent only on overall flow characteristics, such as the total throughput velocity Reynolds number. This force F may then be determined indirectly from experimental measurements of the agglomeration time. The first law of thermodynamics applied to the control volume states that the work done by this force F on the control volume is equal to the energy change of the material in the control volume due to viscous dissipation, and surface energy changes. Assuming that F is known and that the transverse bubble velocities under the action of F obey Stokes' Law, one may obtain a solution for the time needed for the process to become completed as a function of initial bubble population and size.

This model had to be abandoned, however, when the purity effect indicated that considerations of dynamic surface tension, which are not allowed for by the proposed model, are a primary variable in the agglomeration process.

3.2 Bubble Collision Model

The observations made in both the counterflow and the co-current flow experiments justify the following description for the stages of agglomeration:

The first requirement is that a bubble cap be formed somewhere in the tube. This cap is formed after a sufficient number of small bubbles coalesce. The cap formation time may be short or very long depending on properties and flow conditions.

Once a cap is formed, the transition process proceeds very rapidly. The wake behind a cap is practically identical to the wake behind a Taylor bubble (1). Bubbles are axially pulled up in the wake and coalesce with the cap.

It follows, that the process controlling agglomeration is that by which a cap is formed.

Careful observation of a bubble flow, reveals that, even in a relatively dispersed mixture, a large number of bubble impacts occur every second. Most of these impacts result in bouncing-off of the two bubbles with each bubble maintaining its identity. A small number of these collisions, however, results in coalescence of the two bubbles, thus forming one. Further collisions and coalescences of these larger bubbles eventually result in a bubble cap and

hence, rapidly, in a Taylor bubble.

This description suggests that the agglomeration time (or length) is determined by the following two quantities:

1. The number of collisions experienced per bubble per unit time.
2. The probable number of collisions required for coalescence of two small bubbles, or, in other words, the probability of coalescence per collision.

The first of these quantities, the number of collisions, depends on such factors as the bubble concentration, size, and spacing (or volume quality of gas in the mixture), and on flow parameters, such as tube diameter, velocities, or Reynolds numbers.

The second quantity, the fraction of coalescence per collision, depends on what was called in Section 2, the ability of the bubble to resist destruction. Since in some contaminated liquids the concentration of impurities is greater in a surface film than in the bulk of the liquid, the surface tension in the film is non-uniform. Consequently, the interface can resist tangential stresses. This results in a greater ability of the bubble to resist destruction and, hence, tends to reduce the number of coalescences per one hundred collisions. This, then explains why the bubble to slug transition is extremely rapid in a pure liquid but is delayed considerably as some impurities (e.g. salt, soap, etc.) are added.

It follows that in order to describe the transition process adequately, models must be defined which give a measure of the two quantities mentioned above. A proposed model for determining the

number of collisions per unit time is described in the following paragraphs. The probability of coalescence per collision has been studied by means of the two bubble experiment which is described in detail in Section 6.

In the proposed bubble collision model it is postulated that slug flow is essentially reached once a bubble cap of length equal to about ¼ of the tube diameter is formed in the tube. This cap then serves as the nucleus for further development of a Taylor bubble.

If one assumes that bubbles are spheres having a characteristic diameter D_b, and that they are distributed in the tube according to a face-centered cubic lattice, then the gas volume quality, Φ, may be written as

$$\Phi = \frac{\pi}{3\sqrt{2}} \left(\frac{D_b}{\alpha}\right)^3 \tag{1}$$

where α is half the face diagonal in the cubic lattice. Now, the volume to length relation for short Taylor bubbles is given by (18)

$$L_b / D_p = 1.82 \; V_b / A_p D_p$$

whence the volume of a cap of length $D_p / 4$

$$V_b = 0.137 \, A_p D_p$$

Then the number of bubbles of initial size D_b which must agglomerate in order to form a cap is:

$$0.137\, A_p\, D_p = m\, \pi/6\, D_b^3$$

or,

$$m = 0.206\, (D_p / D_b)^3 \qquad (2)$$

The agglomeration of bubbles is due to collisions between them, which in turn are due to random motions of bubbles in the tube. It is assumed that the perturbation velocity of a bubble with respect to others is characterized by a root-mean-square characteristic velocity, $\overline{c}$. This characteristic velocity is governed by such factors as the total throughput velocity of the bubbles, interaction between neighboring bubbles due to wake effects, the oscillating character of the rise of bubbles in a liquid, etc.

The number of collisions per bubble per unit time may be estimated as follows.

According to the assumption that the motion of bubbles is perfectly random while their average positions form a face-centered cubic lattice, each bubble has a sphere of influence whose diameter is equal to $(\alpha - D_b)$ as shown in Figure 4a.

If at each bubble contact, the area of contact between bubble and sphere of influence is $\pi D_b^2/4$, the time required for the entire surface of the sphere of influence to be "touched" by a bubble is

$$\frac{\pi (\alpha - D_b)^2}{\pi D_b^2/4} \quad x \quad \frac{(\alpha - D_b)(1 + f)}{\overline{c}} \qquad (3)$$

In Equation (3), f is a fraction defining the lag time of a bubble at a spot on the influence sphere. The time of contact of a bubble with a spot on the influence sphere is given by

$$\delta_c = f \cdot \frac{(\alpha - D_b)}{\bar{c}} \tag{4}$$

The number of times a bubble in an influence sphere touches a particular collision spot per unit time is given by the inverse of Equation (3)

$$\lambda = \frac{\bar{c}\, D_b^2}{4\,(\alpha - D_b)^3\,(1 + f)} \tag{5}$$

A collision spot is a point on an influence sphere where it is possible for two bubbles to touch. Each sphere has eight such spots. A collision is said to take place when a bubble arrives at a spot at or before the time another bubble left it. According to this definition, the probability that two bubbles are at the same spot in time dt is

$$\lambda\, dt \cdot \lambda(dt + 2\delta_c) = 2\lambda^2 \delta_c\, dt$$

and the probability that the two bubbles are at the same spot per unit time is $2\lambda^2\delta_c$

Hence, the number of collisions per spot per second is, using Equations (4) and (5)

$$\frac{1}{8} \quad \frac{\bar{c}\, D_b^4}{(\alpha - D_b)^5} \quad \frac{f}{(1 + f)^2}$$

Or, using Equation (1) and the fact that there are eight collisions spots per bubble, the number of collisions per bubble per second is obtained

$$\eta = \frac{\bar{c}\, f}{D_b (1+f)^2 \left[\left(\frac{0.74}{\Phi}\right)^{1/3} - 1 \right]^5} \tag{6}$$

The speed of the bubble to slug transition process is proportional to the number of collisions per bubble second. Equation (6) is plotted in Figure 4b. According to Figure 4b, the transition to slug flow is extremely slow (very few collisions per bubble) for void fractions smaller than 8%. With such low void fractions, the flow configuration appears as a "stable" bubble flow even for pure liquids and long flow sections. With void fractions greater than 30%, on the other hand, the transition to slug flow is extremely rapid, even in a contaminated liquid. The actual void fraction at which transition occurs depends, of course, on the number of coalescences per collision. It should be noted that most experimental observations and proposed flow regime maps reported in the literature, place the bubble to slug transition line at a void fraction between 10% and 25% (see for example (12) and (20). This is in excellent agreement with the predictions of Figure 4b.

To complete the analysis of the collision model, the speed of agglomeration depends also on the number of original bubbles needed to form a cap (Equation 2) and on the function of coalescence per collision. The agglomeration time is then

$$t = \frac{0.206}{P} \frac{D_b}{\bar{c}} \frac{(1+f)^2}{f} \left(\frac{D_p}{D_b}\right)^3 \left[\left(\frac{0.74}{\Phi}\right)^{1/3} - 1\right]^5 \quad (7)$$

Equation (7) is intended to be used simply as a guide to the quantities which influence the agglomeration process. It illustrates the qualitative effects of bubble and tube diameters, void fraction and purity. The actual value of the agglomeration time may deviate from that predicted by Equation (7) because of the various idealizations incorporated in the analysis.

4.0 COUNTERFLOW BUBBLE-SLUG TRANSITION OBSERVATIONS

4.1 Apparatus Description

A simple counterflow experiment was erected in order that the mechanism of bubble-slug transition be more clearly defined. This was accomplished by attaching a four foot vertical lucite tube one inch in diameter beneath a two inch diameter tube having a length of one foot. Tap water under pressure was injected into the two inch tube and air through small orifices was introduced at the bottom of the one inch tube (Figure 3). By adjusting the water flow rate, a swarm of bubbles could be held in approximately one section of the one inch tube for any length of time. The two inch diameter tube served as an air-water separator.

4.2 Test Procedure

A swarm of bubbles (nitrogen) with D_t/D_b ratios between 4 and 6 was generated for each test. Initial bubble density and bubble column height were controlled by appropriate gas-water flow rate settings and cutoff periods.

4.3 Qualitative Results

All transitions from bubble flow to slug flow are characterized by a "cap" formation. Bubbles uniformly distributed over a portion of the test tube adjust themselves into bubble packets. Some of the leading bubbles in each packet fix themselves to each other in the form of a cell-structured cap, while the trailing bubbles for that moment continue to move in respect to each other. Under the influence of the cap's wake, layers of bubbles quickly fix themselves to the cap's underside, forming an effective G. I. Taylor bubble. Shortly thereafter, the cell-structured pattern breaks down resulting

in a normal G. I. Taylor bubble. All the packets in the column go through the various stages almost simultaneously.

If well behaved characteristics of this experiment can be extended to co-current flow fields, then the agglomeration point should be a stationary point when inlet conditions remain constant. In summary, bubble to slug transition is characterized by a general grouping together of bubbles, until the formation of a cap, which accelerates the process to completion.

5.0 CO-CURRENT BUBBLE-SLUG TRANSITION APPARATUS

5.1 Apparatus Description

The components of the system are as follows:

5.1.1 Test Section

A 2 inch I.D. lucite tube 21.5 feet high comprises the observation tube. A tape measure along the tube indicates distances from inlet. To support an observer, a scaffold was erected paralleling the tube.

5.1.2 Open Loop Air System

Air supplied from a 150 psig lab source is filtered before entering the system. Components of the system as the air flow encounters them are -- pressure regulator, temperature-pressure tank, flow measuring orifice, flow control valve, a pressure tank with 45 tube inserts, 45 lengths of plastic tubing, and 45 orifice assemblies having final diameters of 0.009 inches at the inlet of the test section. Also, a flow pressure tap is placed at the inlet of the test section to determine, together with mass flow rate readings, the gas volume flow rate.

The flow orifice has been calibrated using a gasometer. Inclined mercury and vertical oil manometers are used respectively for high and low mass flow rates. Temperature measurements in the pressure-temperature tank are made using a chromel-alumel thermocouple. Plastic tubes leading to the orifice assemblies allow any number of them to be made inoperative, thereby producing larger bubbles for a given

volume flow rate.

The inlet geometry had been designed to produce a parallel velocity profile in order to allow each of the uniformly distributed orifices to inject a more uniform bubble size across the inlet section. After having passed through the test section, air is then separated from the water and exhausted to the atmosphere. The system, however, is designed so that the gas phase can be recirculated if desired.

5.1.3 Closed Loop Water System

Water is circulated through the system by means of a brass gear pump. Volume flow rates are measured by a fuel oil rotometer calibrated for water to read gallons per minute. A bypass provides excellent means of varying the water flow rate. Changeable distilled water bottles (5 gals.) serve as water surge tanks.

5.1.4 Inlet-Separator Tanks

The inlet tank supports orifices at the tube entrance and also uses a wire mesh flow screen to dissipate all disturbances in the flow prior to its entering the test section.

Separation of air-water mixture is accomplished at the top of the experiment in a separator tank. Both tanks are made from brass stock.

Schematic diagrams and pictures of the apparatus are included in Figures 6, 7, 8, and 9.

5.2 Experimental Procedure

Before a test, the system is thoroughly flushed with water -- first tap water and then distilled water. Test liquid is then pumped into the system and circulated for half an hour. During this period, a contamination process takes place, and upon its completion the flow field stabilizes for given inlet conditions.

After these initial preparations, the actual data recording commences. While holding the water flow rate constant, for different air flow rates, respective agglomeration points are noted. For each agglomeration point reading, the flow field is allowed to reach steady state (constant inlet conditions and a fixed agglomeration point.)

A complete run includes three different water flow rate settings during each of which the air flow rate is varied to produce various agglomeration points. Before proceeding to the next water flow rate setting, a water sample is taken from the system.

They are in turn used to determine the purity* state of the liquid (more correctly, the bubble coalescence resistance state) and to detect consequently any change in this property during a particular run.

---

* For presentation ease - purity is used instead of bubble coalescence resistance even though the two are not equivalent (see Sections 6.0, and 6.4.1)

Major bubble coalescence resistance (purity) alterations are made by adding different amounts of sodium sulfate to commercially distilled water.

The bubble coalescence resistance measuring technique is described in Section 6.

5.3 Experimental Results

5.3.1. Visual Observations

The bubble to slug flow transition observed with highly pure liquid at low volume qualities is similar to the type of transition described in the counterflow experiment. The transition process begins with the appearance of a cap and is followed by the formation of short (1½ to 2 tube diameters in length) Taylor bubbles. The length of tube traveled from the time of formation of a cap to the formation of a complete Taylor bubble is of the order of 10 to 30 per cent of the entire agglomeration length. However, the cell-structured pattern described in the counterflow experiments (effective Taylor bubbles), are almost non-existent in co-current flow of pure liquid. In general, transition in the case of pure liquids is a rapid process.

The transition process appears to change as the water impurity is increased. An "effective" Taylor bubble is formed at the core of the tube. The diameter of this bubble or cell is of the order of half the tube diameter. This cell eventually grows in diameter and finally forms an actual Taylor bubble. Increasing the impurity of the liquid still

more, higher and higher volume flow rates of gas are required in order to bring the transition phenomenon within the test section. While, on the average, the flow is more stable against bubble coalescence, the agglomeration point begins to float. In addition to this erratic behavior one sees an intermittent sudden collapse of bubble flow to produce Taylor bubbles 50 to 70 tube diameters long. Once this long bubble leaves the tube, the flow pattern returns to a disturbed bubble flow until another collapse takes place. This phenomenon appears to be due to some stability limitation rather than to the transition mechanism described above.

The reproducibility of the agglomeration points is substantiated when two runs having test liquids with approximately equal purity ratings produce compatible experimental results (e.g. runs 2 and 3.)

Water flow rate is an important parameter as might have been expected. However, the agglomeration point sensitivity on water flow rate is most noticeable at low gas rates in high purity liquid. A 5% change in water flow rate produces a 10 - 30% change in the agglomeration length.

Inlet bubble sizes are determined by microflash pictures. When the bubble size is substantially increased, the agglomeration point is observed to descend. However, due to the limited variation in the bubble diameter and the difficulty in accurate diameter measurements, no quantitative evaluations of the

bubble diameter effect were possible.

5.3.2 Quantitative Results

After initial debugging and calibration tests, fifteen complete runs were made on the co-current bubble to slug transition apparatus. The first ten of these were utilized in defining clearly the agglomeration point and in establishing qualitatively the effects of contamination. Once these problems were resolved satisfactorily, the remaining five runs were conducted under well controlled conditions. These five runs constitute the essential data presented in this report.

Time limitations prevented full exploitation of the co-current bubble to slug transition apparatus to include effects of different tube diameters etc. The determination of all the conditions that effect the transition process and hence of the means of attaining reproducibility consumed most of the available time. In fact, the definition of these conditions, even qualitatively, is believed to be one of the most important contributions of this work.

Data from the five runs are presented in Appendix I.

6.0 LIQUID PURITY - TWO BUBBLE EXPERIMENT

6.1 Objectives

When a property of a system is not completely defined, there are two ways to present data involving this property: one is to specify the system's complete history from a known base point; the other is to perform a test on the system which will identify the state of that property. If the transition phenomenon is a weak function of purity or if it is a strong function of only one type of impurity, then specifying the history of the liquid would suffice.

When experiments in co-current transitional process were first contemplated, specifying the history of the liquid seemed to be sufficient. It was anticipated that for purity classification a broad description such as distilled, tap, or soapy water, would be sufficient. However, in practice, this is not the case. The transition phenomenon actually depends upon many chemical and particle impurities, some increasing and some decreasing bubble coalescence resistance.

Therefore, a method was needed by which bubble coalescence resistance can be determined from the liquid itself. The first clue on how this might be accomplished was found in an article by Foulk and Miller (10). The two bubble experiment as it is called, consists essentially of two probes. The top probe holds the bubble while the bottom probe generates bubbles and pushes them against the top bubble. When the bubbles are together, one of two things happen - they coalesce forming one bubble or they do not coalesce and roll-off each other.

Two things should be noted in Foulk's experiments:

1. Bubbles are forced against each other so that they are visually deformed.
2. The bottom bubble is attached to the bottom probe when collision occurs.

Thus, approach velocity is only due to the bubble's growth rate.

Their experimental results show that as the molarity of sodium sulfate increases, the number of coalescences per collision decreases. In the interesting range ($0 \leqslant M \leqslant 0.09$)* of the transition process, less than ten collisions out of one hundred coalesced. However, a simple experiment shows that the coalescences per collision significantly varies as the probes are separated. Thus, a modified two bubble experiment using this phenomenon increases experimental sensitivity and through proper data interpretation, it is capable of indicating bubble coalescence resistance in a liquid.

6.2 Apparatus Description

6.2.1 Probes

The purpose of the bottom probe is to generate bubbles (equal in volume) at a constant rate in order that for a given supply pressure, bubbles are ejected from the probe with the same velocity. The bubbles must also emerge into the liquid at the same location. A design which proved to be most successful incorporates an inclined tube, a cavity, and a holding hole on top of the cavity (Figures 11 and 12).

* Distilled water with sodium sulfate molarity concentrations greater than 0.01 can not support transitional process as defined in Section 2.1.

Inclination and diameter of the inclined tube determines the volume of the bubble to be generated. When the water-air interface in the inclined tube arrives at the cavity, a rapid expansion takes place and the bubble grows until the buoyant forces overcome the surface tension forces in the tube. If the inclination is small (3^{o}), the break will occur at the cavity entrance. If the inclination is large (30^{o}), the break will occur far inside the tube, thereby resulting in large bubbles. Water then rushes in the tube occupying the space vacated by the air. Meanwhile, the bubble being trapped in the cavity (the exit hole being smaller than the bubble diameter) is forced out as the water once again is pushed out of the inclined tube. The general scale is indicated very well in Figures 11 and 12.

The probe is fabricated from 3 mm pyrex glass tubing. A cavity is first blown on the tip of the tube, and when this cools down sufficiently, a well focused flame is directed at the spot where the hole is desired. After a proper waiting period, pressure is applied at the other end of the tube, thereby blowing out the cavity's soften section. Careful firepolishing finishes the hole to proper sizing.

The primary purpose of the top probe is to hold a bubble and retain it after either a coalesced or a non-coalesced collision (Figures 12 and 13). The bubble holder must also release coalesced bubbles as one bubble - allowing no fragments to remain behind.

Both objectives are fulfilled by flaring a tube with a positive curvature (Figures 11 and 12). A carbon rod is formed into a cycloid of revolution on a lathe by a similar shaped tool. The carbon tip is then heated to a high temperature and the tube is revolved on the tip until the desired shape is obtained. The top probe is also made from 3mm pyrex glass tubing.

6.2.2. Air Supply System

Air from a 7 psig laboratory source is reduced in pressure through a needle valve before entering a pressure tank. An inclined mercury manometer registers the tank pressure. From the pressure tank, air travels to the bottom probe through a capillary pressure reduction tube. An air bleed valve, after the needle valve, provides added air flow sensitivity while the manometer indicates any change in the supply tank pressure.

6.2.3. Supporting Structures

The top probe is attached to a vertical traversing rod through clamps and a teflon tube - rod adapter. The traversing rod, calibrated to read 1/100 cm by means of a vernier, in turn is fixed to a two-directional traversing table.

Liquid is contained in a 6 x 6 pyrex glass cylindrical jar. A plexiglass top covers the jar during prolonged testing periods. The bottom probe is fixed to a stand by means of a teflon adapter and is positioned into place by means of universal clamps.

A sighting telescope is used to see more clearly when probes are at zero gap distances and bubble gap distances apart (see

Section 6.3). These two corresponding readings on the vertical traversing rod are null points in the experiment.

A timer and a counter provides means of setting the appropriate bubble generation rate.

A photograph and a schematic of the two bubble experiment is found in Figures 10 and 11.

6.3 Test Procedure

All items in contact with the test water are thoroughly cleaned before each complete test. While testing pure or near pure water, chromic acid is used as the final cleaning agent. Most of the time, a good washing with a chemical soap solution followed by a thorough rinsing is sufficient. All final rinses are made with laboratory distilled water.

The bottom probe is adjusted so that the hole on top of the cavity is horizontal. The top probe is then adjusted until bubbles forming in the inverted cone depart easily from any side of the probe. A "zero gap" reading is then taken after the jar has been filled with 1500 ml of the test liquid. "Zero gap" is a term used to designate that the silhouette gap between the top and the bottom probe is zero, while "bubble gap" is the distance between the top and bottom probe when the top probe holds a bubble and the bottom probe silhouette just touches the bubble being held.

Setting the bubble rate at 36 bubbles per minute, the top probe is eased into a position where the maximum number of coalescences per collision are observed. The vertical traversing rod reading and the percentage of coalescences are recorded. Many

similar readings are taken until the gap range is fully covered. At the conclusion of the test, zero gap and bubble gap readings are noted.

6.4 Quantitative Results

In the two bubble experiment for a given solution, the percentage of bubble coalescence is a function of distance separating the probes. While the percentage of coalescences is not a unique function of the "gap" distance, the area defined by Equation (8) is not only a unique function of sodium sulfate molarity concentration*, but it is also well behaved, measurable and reproducible.

$$A = \int_{S_L}^{S_U} f(s) \quad ds \tag{8}$$

where f (s) is bubble coalescence as a function of gap distance for a constant bubble generation rate.

6.4.1. Distilled Water and Sodium Sulfate

To investigate behavior characteristics of the area defined by Equation (1), a controlled experiment was conducted using laboratory distilled water and reagent sodium sulfate. Before presenting the results, the probe gap distances S_L and S_U will be defined.

When water is pure, 100 per cent coalescences points exist even for gap distances under ½ bubble diameter. However, if the water has a high sodium sulfate molarity concentration (e.g. 0.02), bubbles will not coalesce at small gap distances

* for a particular liquid

and, therefore, must squeeze out in order to escape. Since this squeezing out process varies so much, a distance of 0.26 cm defines the minimum gap distance or S_L. At this distance, bubbles are relatively free to slip around the stationary bubble if they do not coalesce.

The upper gap limit S_U is defined according to the pure water coalescence curve. A pure water coalescence curve stays at 100 per cent until at some gap distance S_1 where there is a sudden drop to 5% in ΔS, ($\frac{\Delta S}{S_1} \rightarrow 0$). To simplify data recording, this steep negative slope is extended to the abscissa. This intersection is defined as S_U and is equal to 0.86 cm. Tests were conducted with various sodium sulfate concentrations. The resulting bubble coalescence resistance indicator areas are plotted against sodium sulfate molarity readings (Figure 14). A planimeter performs the Equation (8) integrations. With the exception of two points, the data falls on a straight line.

At certain molarity concentrations, the coalescence curve produces two sections where the coalescence is 100% (Figure 15). When a bubble leaves the bottom probe, it accelerates until a terminal velocity is reached. Therefore, separating the probes actually increases the collision velocity. Meanwhile, another parameter is varied as the probe is separated, namely the bubble geometric configuration (Figures 12 and 13). This allows the existence of two 100% sections in a coalescence curve. It is quite possible that a spherical geometry requires a different velocity spectrum than a pancake geometry in order

to assure coalescence. To pursue this topic further, a model of two colliding bubbles is necessary (Figure 16).

If two bubbles approach each other with almost zero velocity, the liquid between the two effective interfaces (x) offers almost zero resistance to being squeezed out. Therefore, the bubbles continue to move toward each other until $x = 0$. At this point, the two interfaces are in contact, and the time they remain in contact will be designated as "contact time." If the bubbles are in a gravitational field and the top bubble is fixed, then the force pushing these interfaces together is the buoyant force on the bottom bubble. Under this force, there is a critical contact time for that particular interface which is required before the bubbles can coalesce. The bottom bubble is in an unstable condition and after a certain average time, it will roll off under the buoyant force action. However, if the possible contact time is always greater than the critical contact time, the bubbles will always coalesce. Assume for the moment, that this is the situation existing in Section I of Figure 16.

As the gap is increased, the lower bubble approaches the top bubble with greater velocities than in Section I. Likewise, the resistance to squeeze out the liquid film between the interfaces increases, and more and more of the time before the bubbles separate is required to eliminate the film. Consequently, the possible contact time starts to fall beneath the critical contact time, resulting in non-coalescing collisions. Assume

that this is the general state existing in Section II in Figure 16, and that the colliding bubbles are geometrically more round than flat.

Now increase the gap distance even more and assume that this increase is great enough so that the bottom bubble has a pancake geometric shape as it approaches the top bubble (Figures 12 and 13). While the resistance to squeeze out the liquid film has probably increased substantially over Section II, the geometry is much more stable than round bubbles. Thus, after the forward motion has ceased, bubbles can still expand a good portion into round geometries before rolling off each other. During this time, the remaining liquid film could be squeezed out and enough time could be left so that the possible contact time once again is always greater than the critical contact time, thereby producing 100% bubble coalescences.

This is a plausible explanation of the coalescence-gap distance curve in Figure 15, but it does not answer the more basic questions, for example, "What is the mechanism of bubble coalescence and how does each parameter influence the phenomenon?"

In reference to the first question, it is normally accepted that breakdown or destruction of the interface in a liquid occurs when two interfaces influence one another and thus share one interface which is dynamically and statically unstable.

The reluctance for interfaces to fuse together is a well-known factor in the stability of "touching" soap bubbles. This stability is "probably due to the reluctance of absorbed molecules to rotate and compress themselves." (21) However, aside from this qualitative observation, extension of this reasoning is not discussed in this work. Other parameters, such as dynamic surface tension and the second coefficient of surface tension (Section 2), are believed to influence the bubble rise velocity, the bubble geometric shape, and the surface forces. But to what degree these parameters effect the bubble coalescence phenomenon is not fully known. However, only with the complete understanding of the collision-coalescence phenomenon can the bubble to slug transitional process be resolved. It is to this end that parameters involving the coalescence of two bubbles are discussed in this work.

6.4.2. Distilled Water, Sodium Sulfate and Other Contaminants

In Section 5.2., a brief mention is made concerning a contamination process involving the circulation of the test liquid for the first half an hour in the co-current bubble-slug transition apparatus. When the test liquid begins to circulate in the system, the agglomeration point is much higher then at some time later. Therefore, the resistance to bubble coalescence seems to decrease during this process while all other flow variables are held constant. This phenomenon is manifested using both pure and non-pure (concentrations of

sodium sulfate) liquids. Some of the data definitely demonstrates this effect (Table I - Run I) when not enough preliminary circulation time was given to the system. The immediate questions - "could the two bubble experiment detect this effect and could this effect be reproduced outside the co-current bubble-slug apparatus?" will be discussed in the following paragraph.

First, water samples from the corresponding steady state runs in the co-current bubble-slug transition apparatus produces larger bubble coalescence resistance indicator areas (A) than the controlled tests in Section 6.4.1. for the same molarity concentrations (Figure 14). Recalling that smaller areas (A) indicate greater resistance to bubble coalescence, the two bubble experiment result, therefore, agrees with the co-current transition apparatus observations.

The cause of such behavior is narrowed down around surface contaminates inherent in the apparatus material itself. It is found that a process involving water and air flowing intermittently over a lucite surface produces a water base from which areas (A) are larger than areas (A) for non-treated water at the same sodium sulfate concentration (Figure 14).

However, differences between lucite-treated and non-treated water in the pure or near pure range is small, using the area (A) as defined by Equation (8) and the limits S_L, S_U, as defined in Section 6.4. Coalescence data, instead of leveling

off at 5% at large gap distances with non-treated water, begins to level off at 20% with lucite treated water. To take this effect into account, the upper limit (S_U) is redefined as 1.63 cm.

Area versus sodium sulfate molarity concentrations resulting from lucite treated water and using 1.63 cm as the upper limit (S_U) is found in Figure 17.

Although no controlled experiments were conducted varying particle purity, during the fourth run in the co-current apparatus, a noticeable amount of rust entered the system after the points 4.1 to 4.7 (Appendix I) were recorded.

Two bubble experiment results show that the rust increased the bubble coalescence resistance as though the salt molarity concentration of the test liquid was increased by 0.02.

7.0 AGGLOMERATION LENGTH CORRELATIONS

7.1 "Collision Model" Method

Equation (7) in Section 3.2 states that the agglomeration time is a function of bubble diameter, pipe diameter, void fraction, characteristic velocity, lag time factor (f) and a bubble coalescence fraction (P). If all the parameters except one in Equation (7) are specified, it is then possible by observing the behavior of the floating parameter to judge whether or not Equation (7) basically describes the transition process. To investigate this possibility, the parameters of Equation (7) are evaluated in the following manner.

Agglomeration time is calculated using

$$t = L / \bar{V}_b$$

where $\bar{V}_b = V_d + V_c + 0.8$

Bubble diameter is determined from microflash pictures (Figure 21) taken at the inlet, and on the average, the bubble diameter equals 3.8 mm or 0.15 inches.

The pipe or tube diameter is equal to 2 inches.

Volume void fraction is determined using an equation suggested by Graham Wallis (4),

$$V_d = \bar{\phi} (1 - \bar{\phi}) C_1 + \frac{\bar{\phi}}{(1 - \bar{\phi})} V_c$$

where C_1* is a constant equal to 0.66. The coalescence fraction (P) is some average number of coalescences per one hundred collisions which takes into account the bubble coalescence resistance (purity),

---

* For further reference, see Appendix III

the average impact angle, the average collision velocity and the average time the bubbles are together. In order to evaluate P, a complete analysis of the collision of two bubbles (Section 6.4.1.) is required. However, this analysis would be extremely involved and it is considered at this time prohibitive.

Another approach to evaluating P is to assume that P = F (A) or that P is a function of the area from the two bubble experiment. Inspection of the data trends indicates that a reasonable function is:

$$P = \left(\frac{A}{A_o} \right)^{\frac{1}{2}}$$

where A_o is a normalizing factor which is equal to 0.80 cm and corresponds to the area of pure water, lucite treated, as defined by Equation (8) using lower and upper limits as 0.26 cm and 1.63 cm.

Going one step further, assume the mean contact time of two bubbles to be approximately equal to the collision period, i.e. assume that (f) is equal to one. This leads to a graph in Figure 19 which plots characteristic velocity as a function of A noteworthy feature of this curve is the realistic and well behaved values of $\bar{C}$. The characteristic velocity is of the order of 1 ft/sec for a dispersed mixture and rapidly approaches zero as the mixture becomes increasingly packed. This result strongly suggests that Equation (7) basically describes the transition from bubble flow to slug flow. It is also believed that with more experimental data, quantities like f, etc. can be resolved more completely. Equation (7) and experimental data points (using $\bar{C}$ in Figure 19) are plotted in Figure 20.

7.2 Exponential Correlation

An exponential equation with two floating variables is fitted to curves (L vs. V_d) of constant superficial liquid velocity and bubble coalescence resistance areas.

The final result is of the form:

$$L = 6.0 \; e^{- m_1 (V_d - y)} \tag{9}$$

where

$$m_1 = - 1.39 \; e^{- 1.30 \, V_c} \; \ln A^* + 6.6 \; e^{- 2.04 \, V_c}$$

$$y = \left[0.151 - 0.123 \; e^{- 4.0 \, V_c} \right] \ln A^* + 0.25 \left(1.0 + 1.1 \; \frac{V_c}{0.22} \right)$$

$$A^* = 1 - \frac{A}{0.779}$$

The above equation correlates the data to within $\pm$ 7%. The exponential form is used so that the respective L vs. V_d curves behave well for L greater than 21 feet (e.g. at L = 40 feet, V_d should be within $\pm$20% of the actual values).

7.3 Summary of Test Variables

a.) Tube: 2" Inside diameter - lucite

b.) Bubble: 3.8 mm diameter
+ 10% at high gas flow rates
- 10% at low gas flow rates

c.)	Liquid:	Distilled water with different amounts of sodium sulfate concentrations "Lucite treated" (See Section 6.4.2.)
d.)	Gas:	Air - dehydrated and filtered
e.)	Superficial Liquid Velocity Range:	0 to 0.44 ft/sec
f.)	Superficial Gas Velocity Range:	0 to 0.80 ft/sec
g.)	Inlet Conditions:	Uniform liquid velocity profile, uniform bubble density.

8.0 SUMMARY AND CONCLUSIONS

This report presents experimental measurements and an analytical description of the two phase transition process from bubble flow to slug flow in a vertical pipe.

Preliminary visual observations in both countercurrent and co-current gas-liquid flow systems have indicated that the first requirement for transition to slug flow is that a bubble cap be formed somewhere in the tube. This cap is formed after a sufficient number of small bubbles coalesce. Once a cap is formed, the transition process proceeds rapidly to slug flow. Therefore, the process governing the transition to slug flow is the formation of a cap.

Careful bubble flow observations reveal that even in a relatively dispersed mixture, a large number of bubble collisions occur every second. Most of these result in the bouncing-off of the two bubbles with each maintaining its identity. A small number of these collisions results in coalescence.

This description suggests that the agglomeration time is determined by the following two quantities:

1. number of collisions experienced per bubble per unit time
2. the probability coalescence per collision.

An analysis presented in Section 3.2. results in an equation which predicts the number of collisions per bubble per second as a function principally of the void fraction Φ. The dimensionless

collision frequency is shown plotted against void fraction in Figure 4b.

The probability of coalescence per collision has been studied experimentally by means of the two bubble experiment (Section 6) in which the number of bubble coalescences per one hundred collisions were measured in liquids with variable purity.

The combination of the bubble collision analysis and the two bubble experiment results in the following equation for the agglomeration time

$$t = \frac{0.206}{P} \frac{D_b}{\bar{c}} \frac{(1+f)^2}{f} \left(\frac{D_p}{D_b}\right)^3 \left[\left(\frac{0.74}{\phi}\right)^{1/3} - 1\right]^5 \qquad (7)$$

Experimental measurements of the agglomeration time exhibit some trends as suggested by Equation (7). The experimental data is compared with Equation (7) in Figure 20. For this comparison, the bubble contact time is assumed equal to collision period ($f = 1$). The characteristic velocity C is found in Figure 19.

The experimental data is also correlated by means of an empirical relation in Equation (9).

The conclusion of the present investigation may be summarized as follows:

1. The bubble to slug flow transition is due to collisions between small bubbles with a fraction of these collisions resulting in coalescences. This process continues until a bubble cap is formed.

2. The number of collisions resulting in coalescences usually decreases as impurities are introduced in the liquids. Consequently, extremely pure water (as that used in nuclear reactors will show a much more rapid transition to slug flow than ordinary tap water.
3. When the void fraction is smaller than 10%, the collision frequency is extremely low (Figure 4b). Consequently, bubble flow at smaller than 0.10 appears as a stable flow regime even when the purity is high. Conversely, the collision frequency increases extremely rapidly above $\bar{\Phi}$ = 25% so that transition to slug flow is rapid even in a strongly contaminated liquid.
4. As indicated by Equation (7), the agglomeration time increases with increasing tube diameter and decreases with increasing bubble diameter. It follows that small diameter channels will show slug flow at lower qualities than larger channels. Similarly, slug flow is less likely in high pressure systems (low D_b) than in systems at atmospheric pressures.

NOMENCLATURE

A	Bubble coalescence resistance area - (cm) (See Equation 8)
A_o	Normalizing factor = 0.80 cm
A_p	Cross section area of pipe (ft^2)
C	Characteristic bubble velocity (ft/sec)
C_1	See Equation 11
D_b	Bubble diameter (ft)
D_p	Pipe diameter (ft)
f	Lag time factor for colliding bubbles (See Equation 3)
g	Gravitational acceleration (32.2 ft/sec^2)
L	Agglomeration length (ft)
L_b	Length of G. I. Taylor bubble (ft)
m	See Equation 2
M	Sodium sulfate molarity concentration
n	Number of collisions per bubble per second (1/sec)
n_1	See Equation 11
N_{FR}	Froude number
P	Fraction of bubble collisions resulting in bubble coalescences (See Equation 7)
Q_g	Gas volume flow rate (ft^3/sec)
Q_f	Liquid volume flow rate (ft^3/sec)
S	Probe gas distance (cm)
S_L	Probe lower limit (cm)
S_U	Probe upper limit (cm)
t	Agglomeration time (sec)

v_b	Volume of G. I. Taylor bubble (ft^3)
V_c	Q_c/A_p superficial velocity of continuous phase (liquid) (ft/sec)
V_d	Q_d/A_p superficial velocity of discontinuous phase (gas) (ft/sec)
x	See Figure 16
α	See Figure 4a
δ_c	Contact time of a bubble with a "spot" (sec) (See Equation 4)
λ	See Equation 5
Φ	Void fraction

REFERENCES

1. Moissis, R. and Griffith P., "Entrance Effects in a Two Phase Slug Flow," A.S.M.E. Journal of Heat Transfer, February, 1962.

2. Nicklin, D. J. and Davidson, J. F., "The Onset of Instability in Two-Phase Slug Flow," Institution of Mechanical Engineers, Thermodynamics and Fluid Mechanics Group, Symposium on Two-Phase Fluid Flow, Paper 4, London, February, 1962.

3. Bankoff, S. G., "A Variable Density Single-Fluid Model for Two-Phase Flow with Particular Reference to Steam-Water Flow," Journal of Heat Transfer, November, 1960.

4. Wallis, G. B., "Some Hydrodynamic Aspects of Two-Phase Flow and Boiling," International Heat Transfer Conference, Boulder, Colorado, 1961.

5. Adam, N. K., "The Physics and Chemistry of Surfaces," Oxford, Clarendon Press, p. 129, 1938.

6. Edser, E., British Ass. Adv. Sc., 4th Report on Colloid Chemistry, Vol. 4, p. 264.

7. Ewers, W. E. and Sutherland, K. L., "The Role of Surface Transport in the Stability and Breakdown of Foams," Div. of Industrial Chemistry, C.S.I.R.O., Melbourne, 1952.

8. Scriven, L. E., "Dynamics of a Fluid Interface," Chem. Engineering Science, Vol. 12, p. 98, 1960.

9. Boussinesq, J., "Vitesse de la chute lente, devenue uniform, d'une goutte liquide spherique, dans un fluide visqueux de poids spherique moindre," Comptes Rendus, Vol. 157, p. 313, 1913.

10. Foulk, C. W. and Miller, J. N., "Experimental Evidence in Support of the Balanced-Layer Theory of Liquid Film Formation," Indust. and Engineering Chemistry, p. 1283, Nov. 1931.

11. Kozlov, B. K., "Types of Gas-Liquid Mixtures and Stability Boundaries in Vertical Tubes," Zhur Tech Fiz, Vol. 24, No. 4, p. 656, 1952.

12. Griffith, P., "Two Phase Flow in Pipes," M.I.T. Summer Session Notes, 1962.

13. Moissis, R., "Transition from Slug to Homogeneous Two Phase Flows," Submitted to A.S.M.E. Transactions, Journal of Heat Transfer (Paper 62-H-48).

14. Lamb, H., Hydrodynamics, Dover Publications, New York, 1932.

15. Kynch, G. J., "The Slow Motion of Two or More Spheres Through a Viscous Fluid," Journal of Fluid Mechanics, p. 193, April 1959.

16. Hasimoto, H., "On Periodic Fundamental Solutions of Stokes Equations and Their Applications to Viscous Flow Past Cubic Array of Spheres," J. Fluid Mechanism, Vol. 5, Part 2, p. 317, February, 1959.

17. Verschoor, H., "Some Aspects of the Motion of a Swarm of Gas Bubbles Rising Through a Vertical Liquid Column," Inst. Chem. Eng., Vol. 28, p. 32, 1950.

18. Moissis, R. and Griffith, P., "Entrance Effects in a Developing Slug Flow," Technical Report No. 18, Division of Sponsored Research, M.I.T., January, 1960.

19. Peebles, P. N., and Garber, H. J., "Studies on the Motion of Gas Bubbles in Liquids," Chem. Eng. Prog., Vol. 49, 1953.

20. Bailey, R. V., Zmola, P. C., Taylor, F. M., and Planchet, R. G., "Transport of Gases thru Liquid-Gas Mixtures," Tulane University and Oak Ridge National Laboratory, Report Available from P. C. Zmola, Combustion Grigg, Inc., Windsor, Connecticut

21. Danielli, J. F., Pankhurst, K. G., and Riddiford, A. C., Surface Phenomena in Chemistry and Biology, Pergamon Press, New York, p. 222, 1958.

APPENDIX I

CO-CURRENT BUBBLE FLOW TO SLUG FLOW TRANSITIONAL DATA

Test Liquid: Distilled Water

Run No.	Sodium Sulfate Molarity Concentration
1	0.000
2	0.010
3	0.010
4	0.020
5	0.082

Column (i) the run index number

Column (ii) the water superficial velocity in ft/sec

Column (iii) the air superficial velocity in ft/sec

Column (iv) the agglomeration length in ft

Column (v) the water sample bubble coalescence resistance area (A) (S_L = 0.26, S_U = 1.63) indicator from two bubble experiment in cm.

Column (vi) the data point rating:

- (t) contamination process transitional point
- (-) questionable
- (+) good

i	ii	iii	iv	v	vi
1.1	0	0.056	21	0.77	t
1.2	0	0.103	16		t
1.3	0	0.167	8		t
1.4	0.22	0.087	20		t
1.5	0.22	0.148	8		t
1.6	0.44	0.056	21.5		+
1.7	0.44	0.073	18.5		+
1.8	0.44	0.098	15.0		+
1.9	0.44	0.120	12.5		+
1.10	0.44	0.146	10.5		+
1.11	0.44	0.173	7.5		+
1.12	0	0.023	21.0		+
1.13	0	0.032	18		+
1.14	0	0.055	14		+
1.15	0	0.071	11		+
1.16	0	0.090	9		+
1.17	0	0.119	6		+
2.1	0	0.095	19.5	0.670	+
2.2	0	0.129	14.5		+
2.3	0	0.080	20.0		+
2.4	0	0.114	16.0		+
2.5	0	0.136	10.5		+
2.6	0	0.164	6.5		+
2.7	0.22	0.170	18.5		+

i	ii	iii	iv	v	vi
2.8	0.22	0.210	13.0		+
2.9	0.22	0.306	7.5		+
2.10	0.44	0.299	18.5		+
2.11	0.44	0.419	14		+
2.12	0.44	0.535	8	0.666	+
2.13	0	0.136	11		+
3.1	0	0.152	15		t
3.2	0	0.183	12		t
3.3	0.22	0.210	21		t
3.4	0.22	0.294	13		t
3.5	0.44	0.268	20.5		+
3.6	0.44	0.296	19		+
3.7	0.44	0.342	17		+
3.8	0.44	0.367	15		+
3.9	0.44	0.460	12		+
3.10	0.44	0.520	10.5		+
3.11	0.44	0.576	9		+
3.12	0	0.076	21.5	0.575	+
3.13	0	0.146	14		+
3.14	0	0.172	11		+
3.15	0	0.195	7		+
3.16	0	0.101	20		+

i	ii	iii	iv	v	vi
4.1	0	0.124	21.5		t
4.2	0	0.188	10.5		t
4.3	0	0.085	21.5		+
4.4	0	0.102	19		+
4.5	0	0.147	14.5		+
4.6	0	0.162	10.5		+
4.7	0	0.179	8	0.480	+
4.8	0.22	0.126	21.5		-
4.9	0.22	0.147	20		-
4.10	0.22	0.172	19		-
4.11	0.22	0.202	16.5		-
4.12	0.22	0.234	14.5		-
4.13	0.22	0.275	11.5		-
4.14	0.22	0.405	8		+
4.15	0.44	0.375	20		+
4.16	0.44	0.440	17.5		+
4.17	0.44	0.487	16		+
4.18	0.44	0.577	11.5		+
4.19	0.44	0.698	7.5	0.22	+

i	ii	iii	iv	v	vi
5.1	0	0.103	20		+
5.2	0	0.136	18.5		+
5.3	0	0.163	14		+
5.4	0	0.175	12.5		+
5.5	0	0.203	7	0.084	+
5.6	0.22	0.229	20		+
5.7	0.22	0.263	18.5		+
5.8	0.22	0.312	15		+
5.9	0.22	0.387	12		+
5.10	0.22	0.433	6.5		+
5.11	0.44	0.543	15		+
5.12	0.44	0.568	11		+
5.13	0.44	0.644	9	0.062	+

APPENDIX II

FIGURES

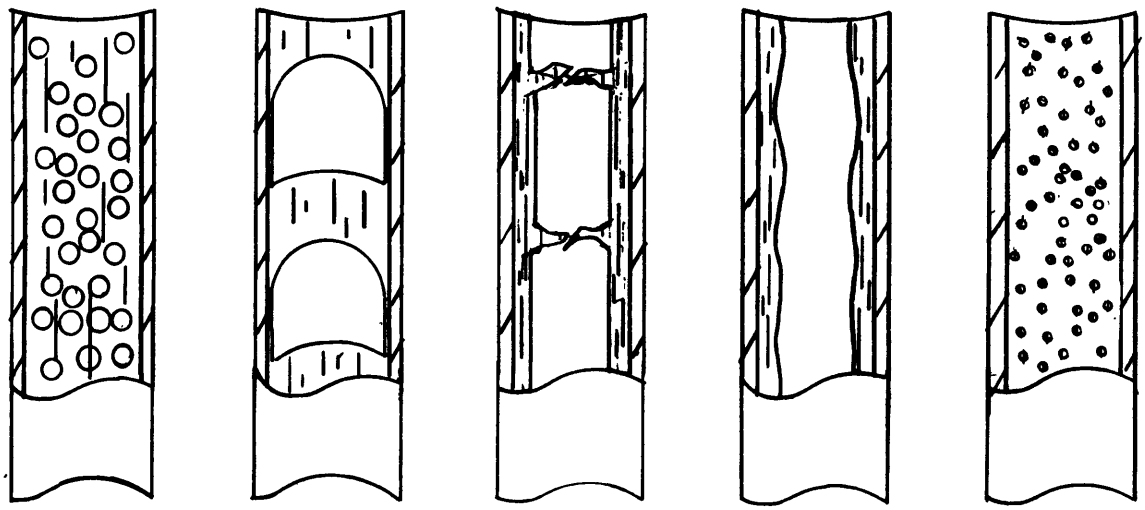

FIGURE 1

FLOW MAP FOR A VERTICAL TUBE

Section I : Bubble Regime
Section II: Slug Regime
Section III: Mist & Annular Regimes

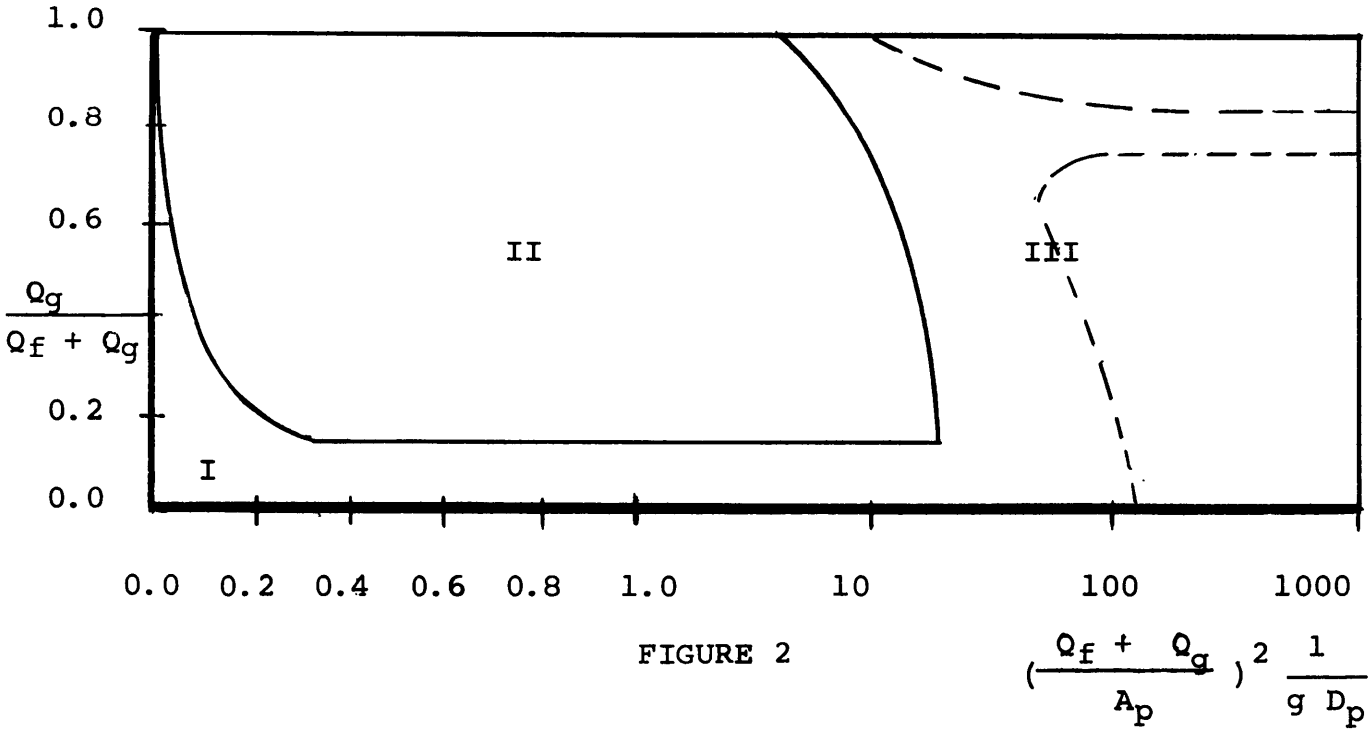

FIGURE 2

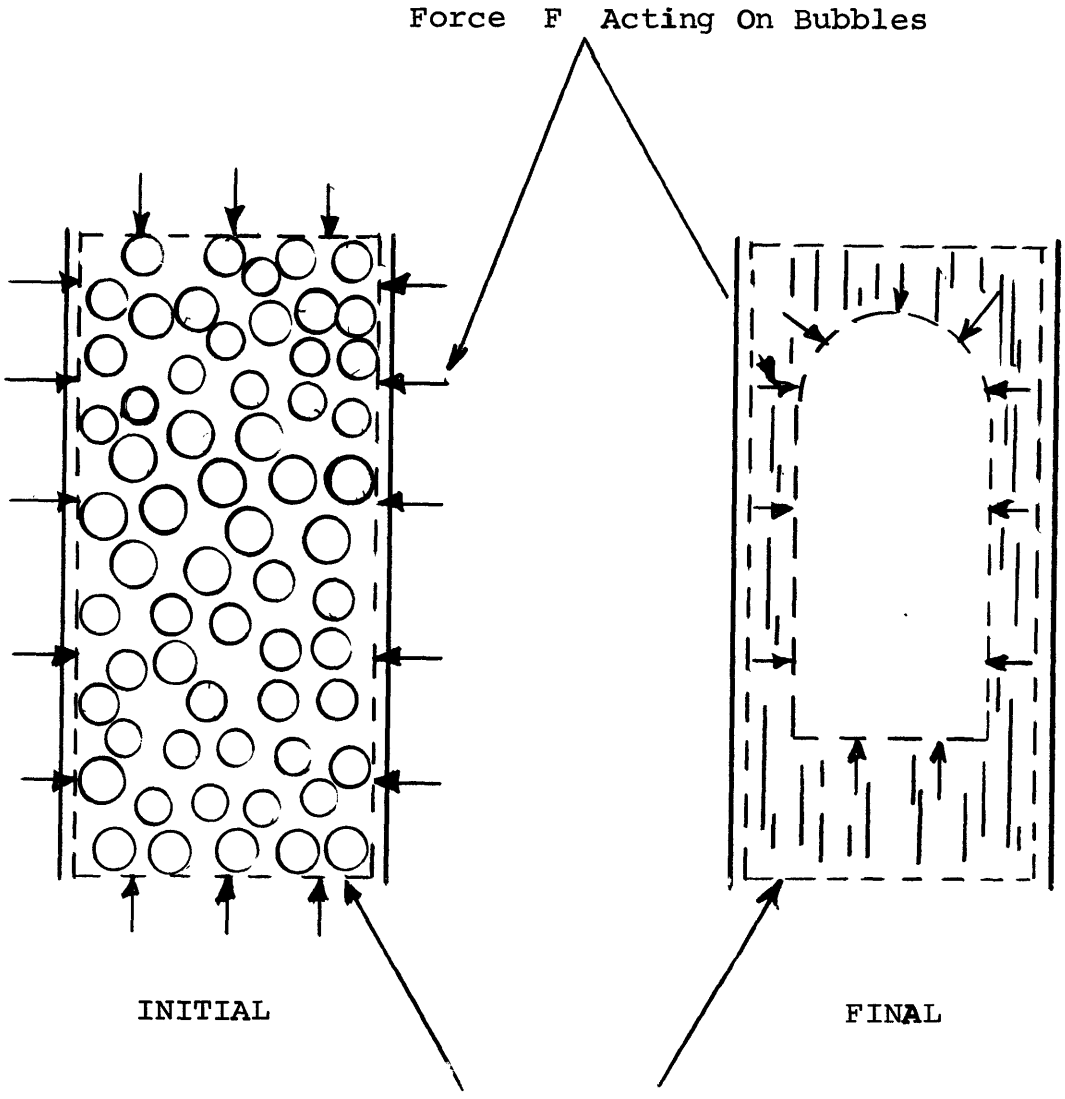

CONTROL VOLUME MODEL

FIGURE 3

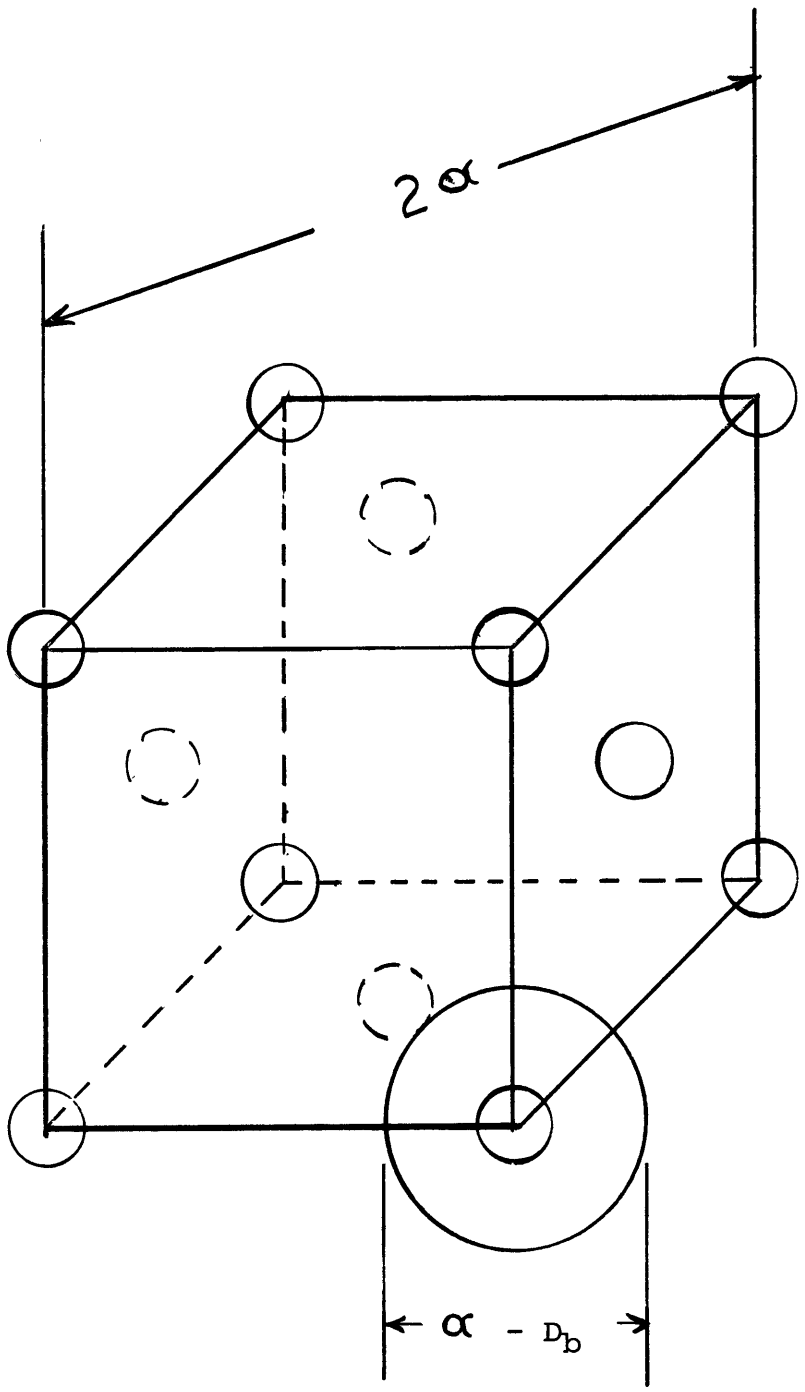

Sphere of Influence

BUBBLE LATTICE ARRANGEMENT AND SPHERES OF INFLUENCE

FIGURE 4a

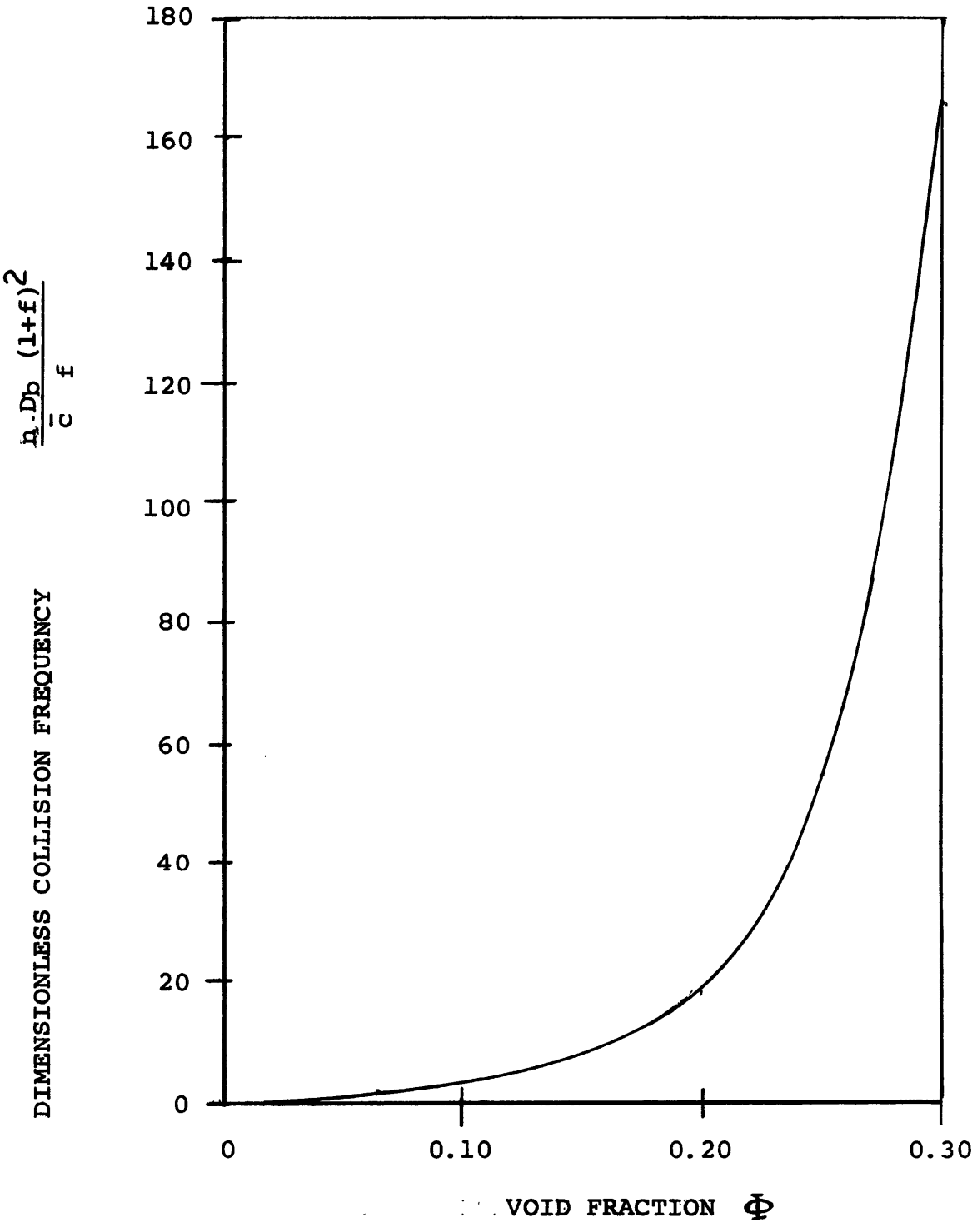

COLLISION FREQUENCY PER BUBBLE

FIGURE 4b

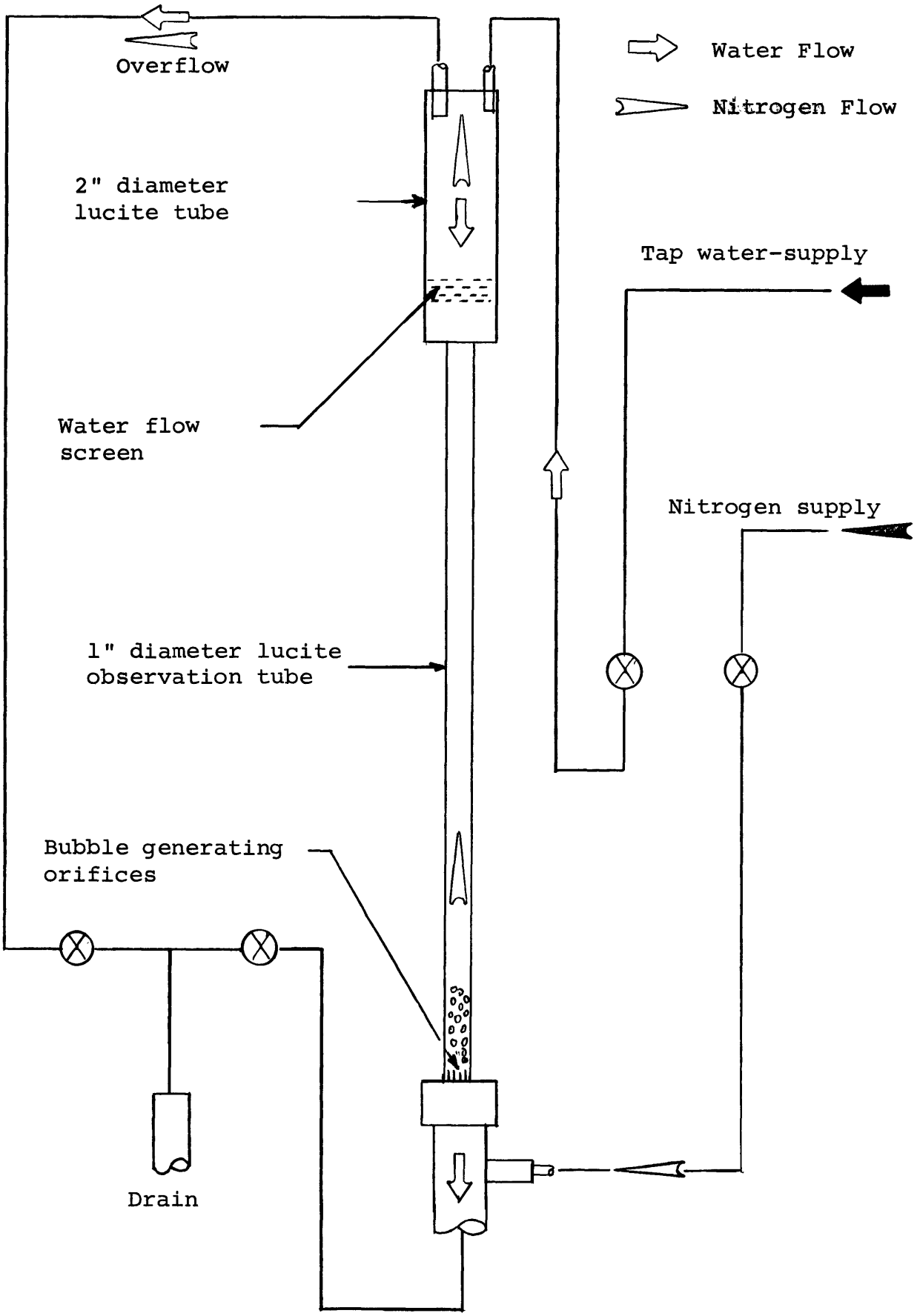

COUNTER-FLOW APPARATUS

FIGURE 5

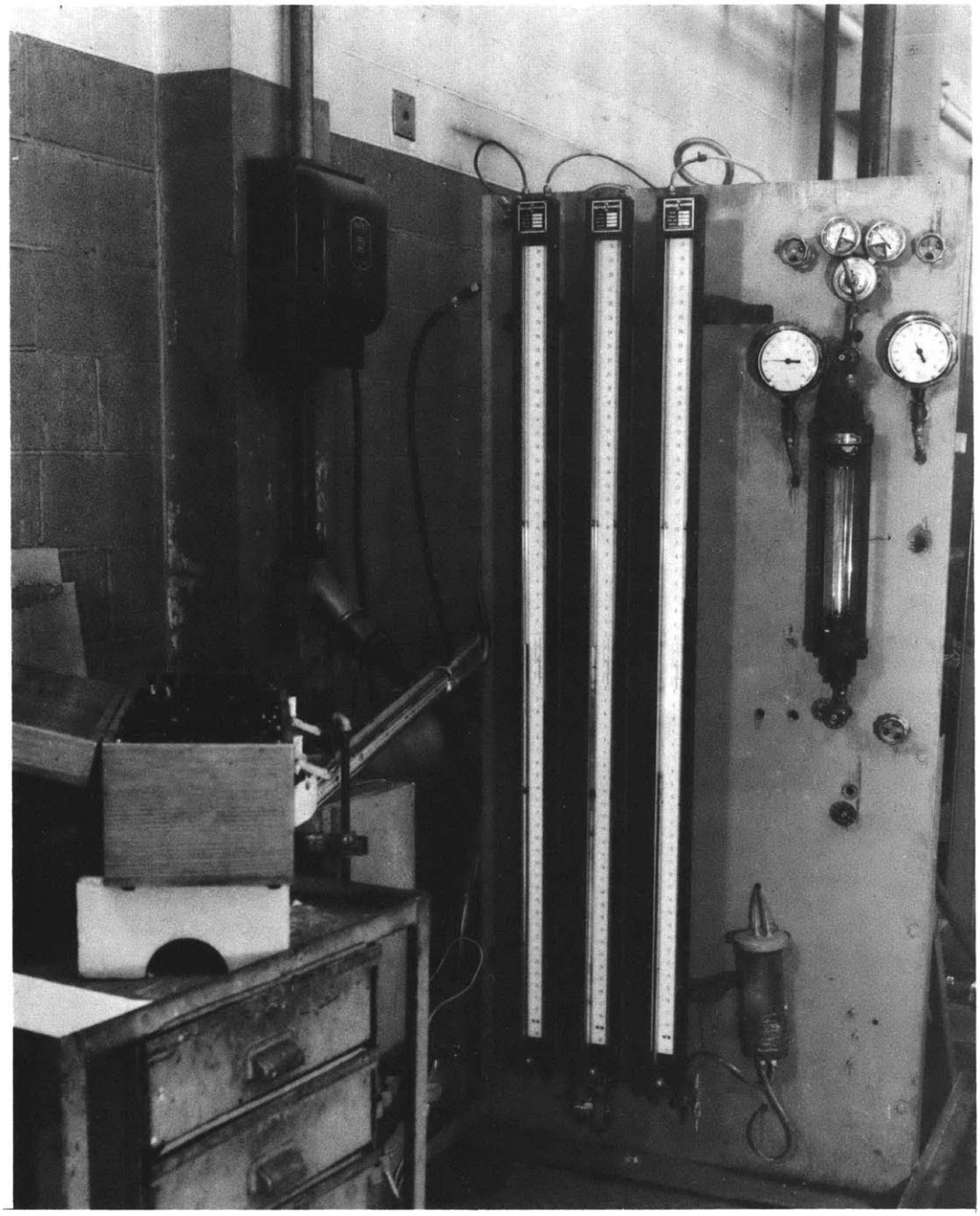

CO-CURRENT APPARATUS INSTRUMENT PANEL

FIGURE 6

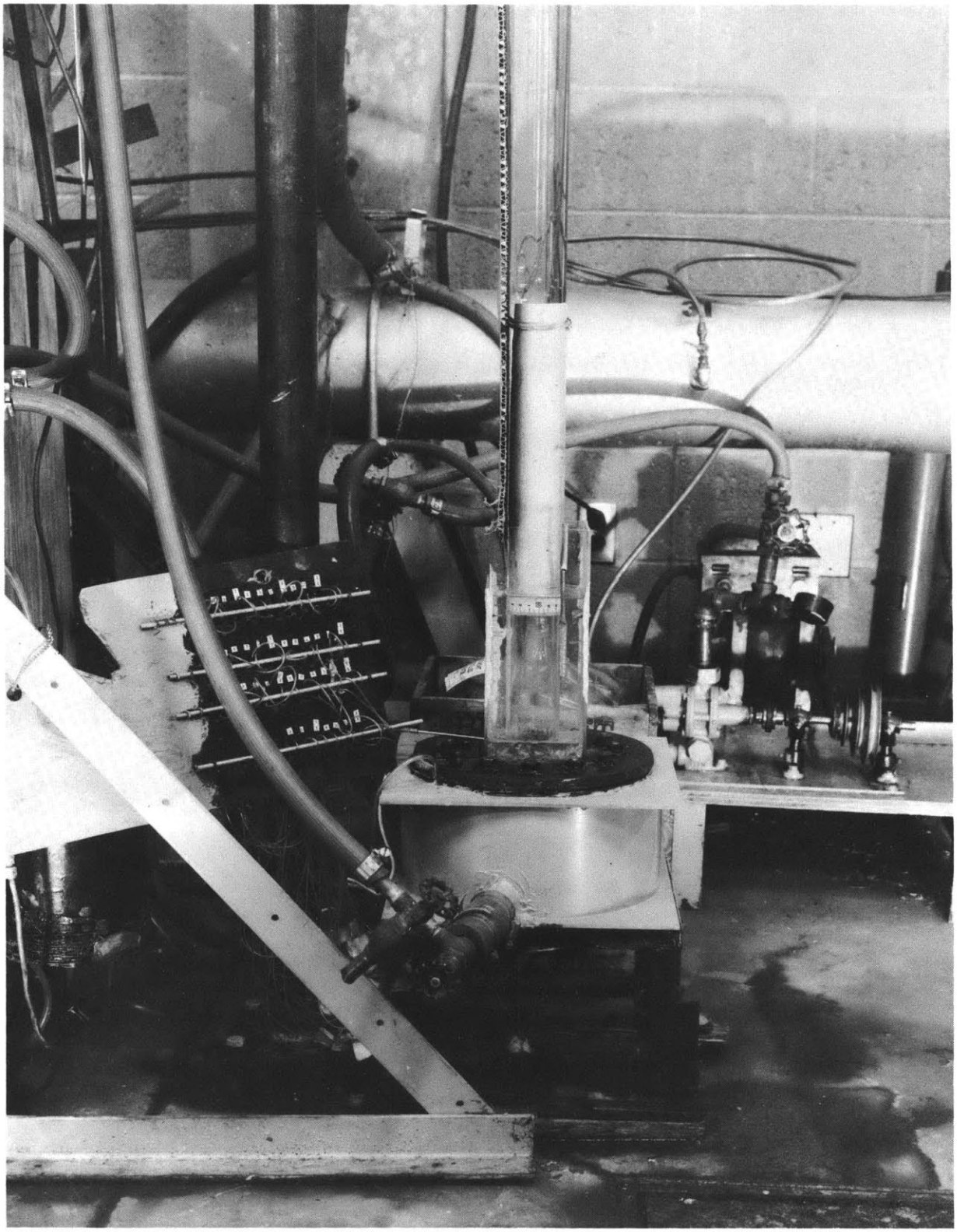

SIDE VIEW

CO-CURRENT APPARATUS

FIGURE 7

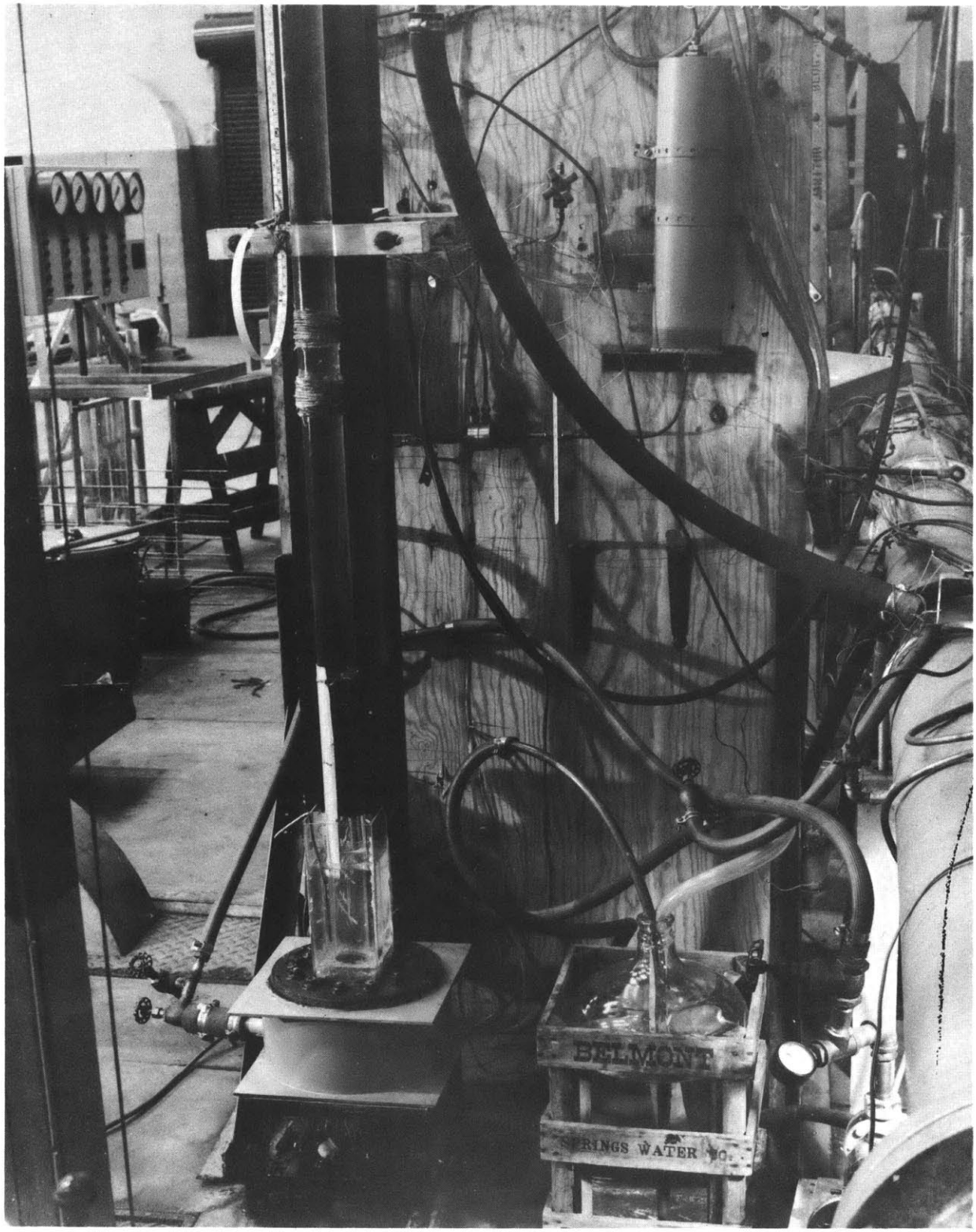

REAR VIEW

CO-CURRENT APPARATUS

FIGURE 8

(A) Motor and water pump
(B) Surge tank (5 gal.)
(C) Water sample bottle
(D) Rotometer
(E) Water bypass valve
(F) Water return pipe
(G) Air-water separator tank
(H) 43 orifices (0.009" diameter)
(J) Inlet tank
(K) Inlet static pressure manometer
(L) Orifice plastic tubing individual flow cut-off panel
(M) Tank - 43 tube inserts
(N) Flow control valve
(O) Flow orifice
(P) Pressure--temperature tank
(Q) Pressure regulator
(R) Air filter and dehydration tank
(S) Thermocouple

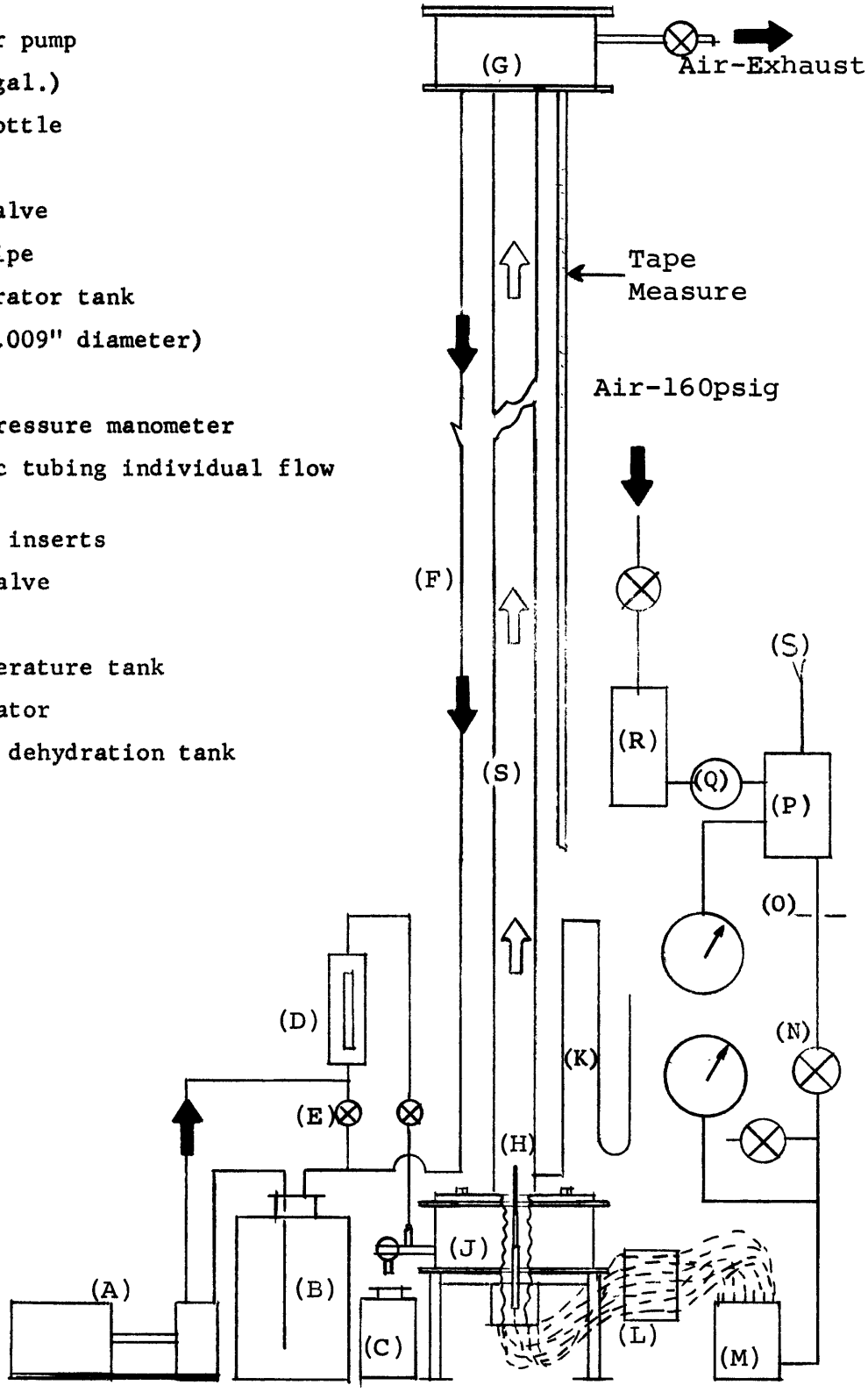

FIGURE 9

CO-CURRENT APPARATUS SCHEMATIC

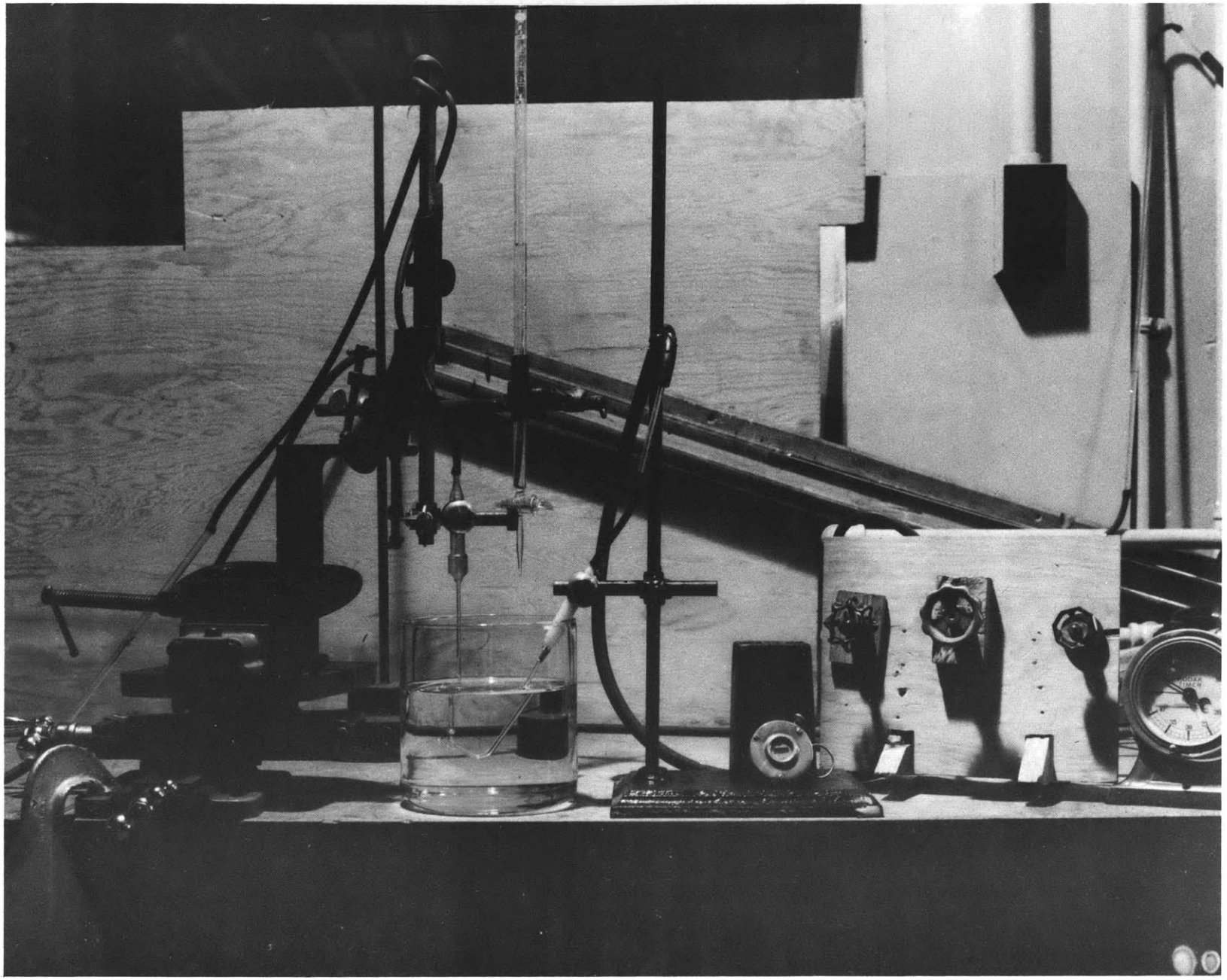

TWO BUBBLE EXPERIMENT

FIGURE 10

(A) Air supply - 7psig
(B) Main control needle valve
(C) By-pass valve
(D) Blow-down valve
(E) Pressure tank
(F) Inclined Mercury manometer

(G) Capillary tube
(H) Bottom Probe
(J) Top Probe
(K) Air-low pressure-source to blow through top probe
(L) Cylindrical jar 6" x 6"
(M) Vertical traversing rod
(N) Vernier scale

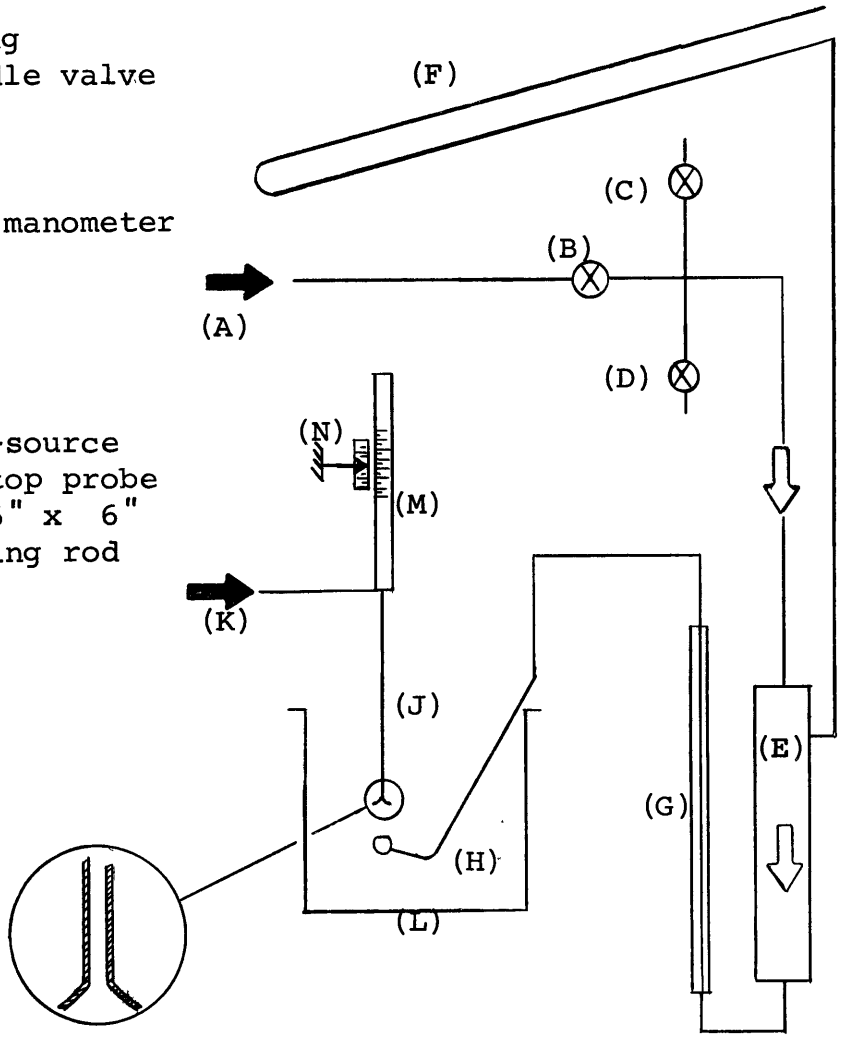

TWO BUBBLE EXPERIMENT

SCHEMATIC

FIGURE 11

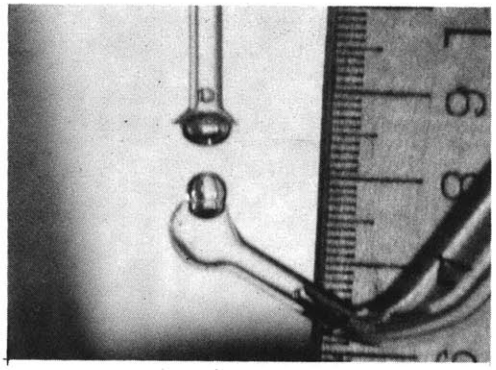

(a)

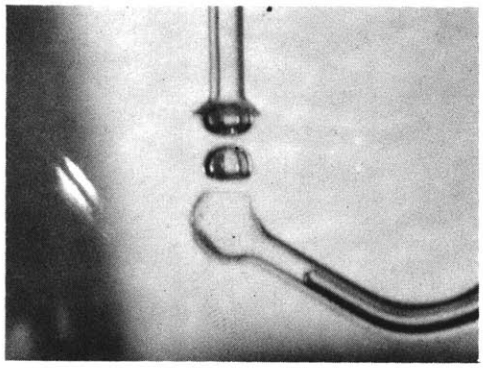

(b)

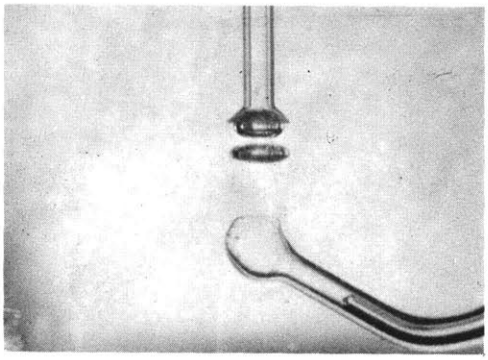

(c)

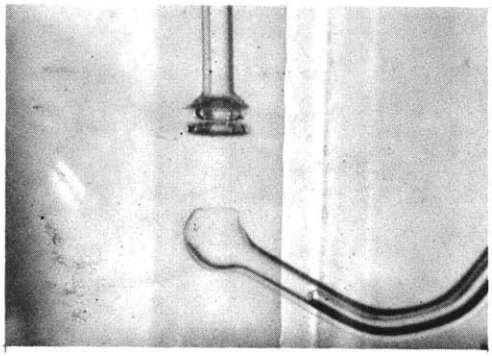

(d)

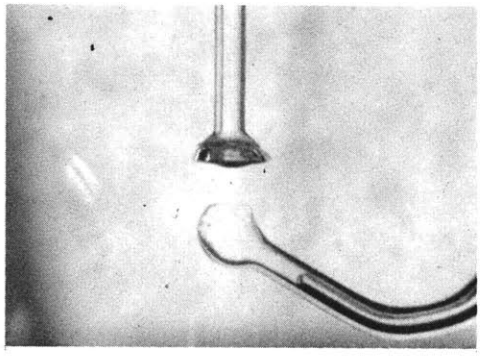

(e)

BUBBLE COLLISION - COALESCENCE IN THE

TWO BUBBLE EXPERIMENT

FIGURE 12

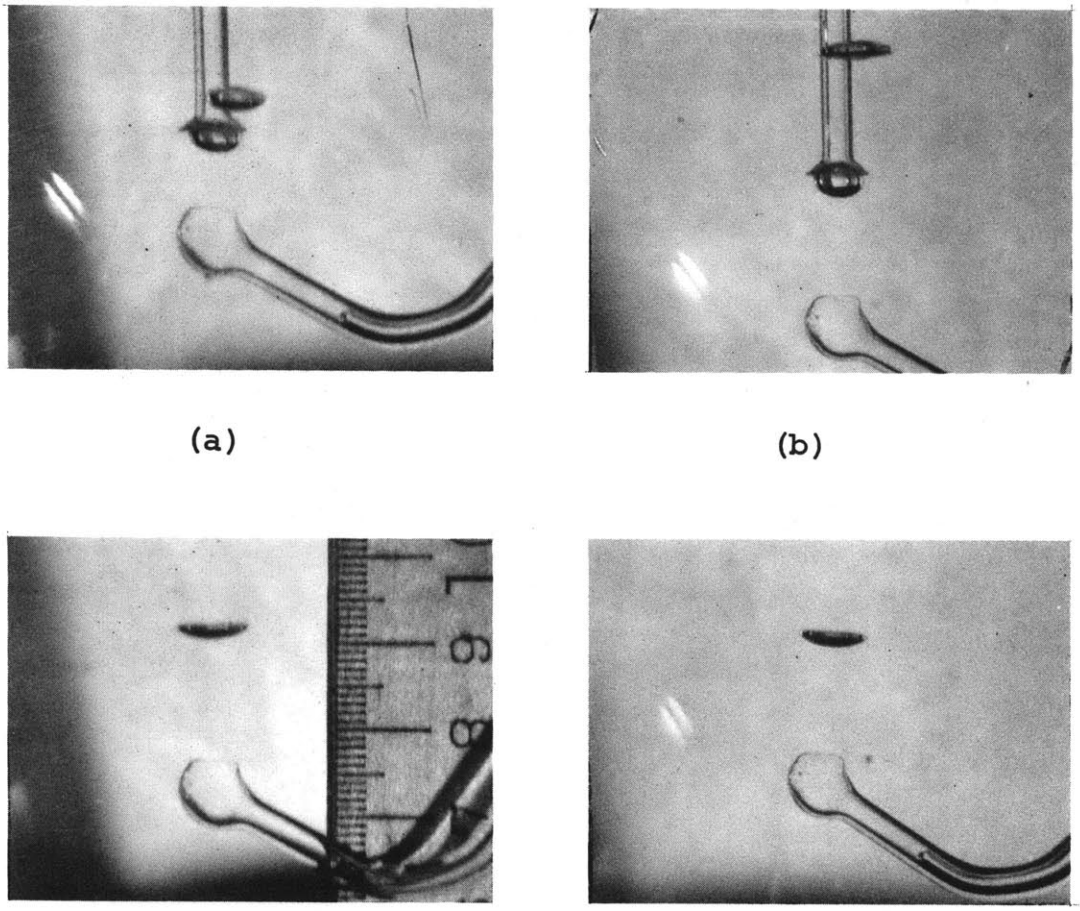

(a) (b)

(c) (d)

a, b, : NON-COALESCENCE BUBBLE COLLISION

c, d, : BUBBLE RISING WITHOUT TOP PROBE

FIGURE 13

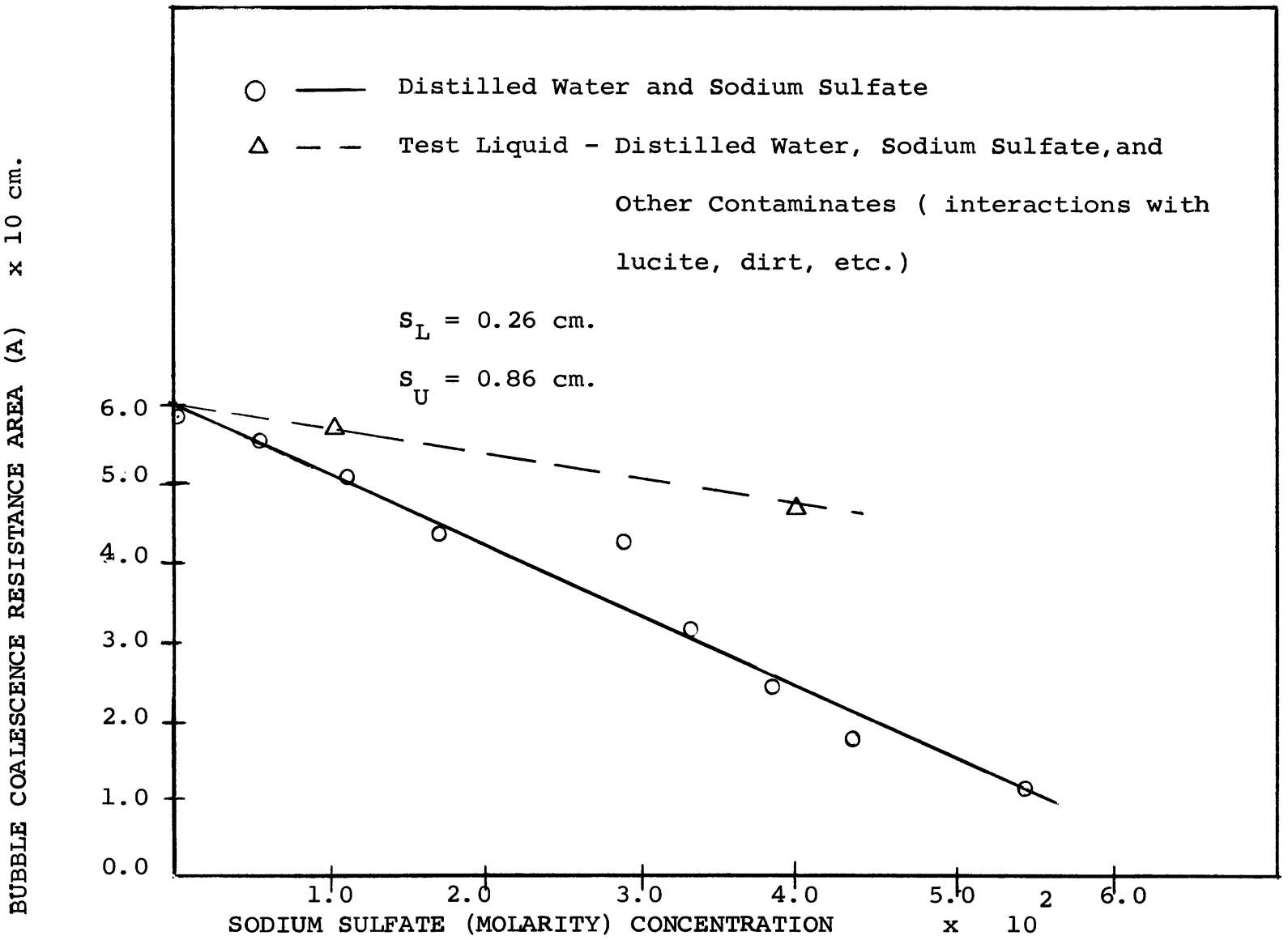
Distilled Water and Sodium Sulfate
Test Liquid - Distilled Water, Sodium Sulfate, and Other Contaminates (interactions with lucite, dirt, etc.)
S_L = 0.26 cm.
S_U = 0.86 cm.
BUBBLE COALESCENCE RESISTANCE AREA (A) x 10 cm.
6.0
5.0
4.0
3.0
2.0
1.0
0.0
1.0
2.0
3.0
4.0
5.0
6.0
SODIUM SULFATE (MOLARITY) CONCENTRATION x 10 2

FIGURE 14

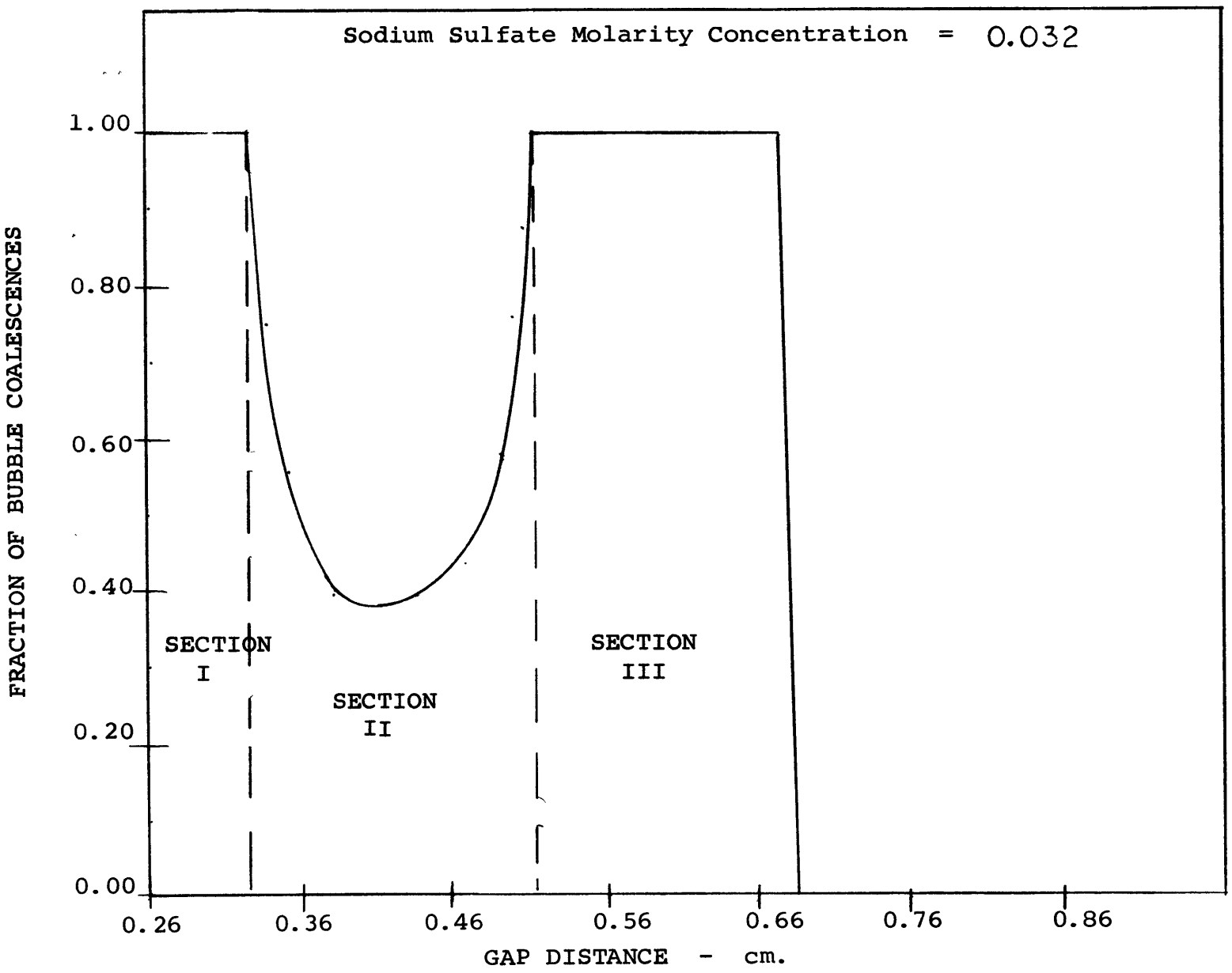
Sodium Sulfate Molarity Concentration = 0.032
FRACTION OF BUBBLE COALESCENCES
1.00
0.80
0.60
0.40
0.20
0.00
SECTION I
SECTION II
SECTION III
0.26
0.36
0.46
0.56
0.66
0.76
0.86
GAP DISTANCE - cm.

FIGURE 15

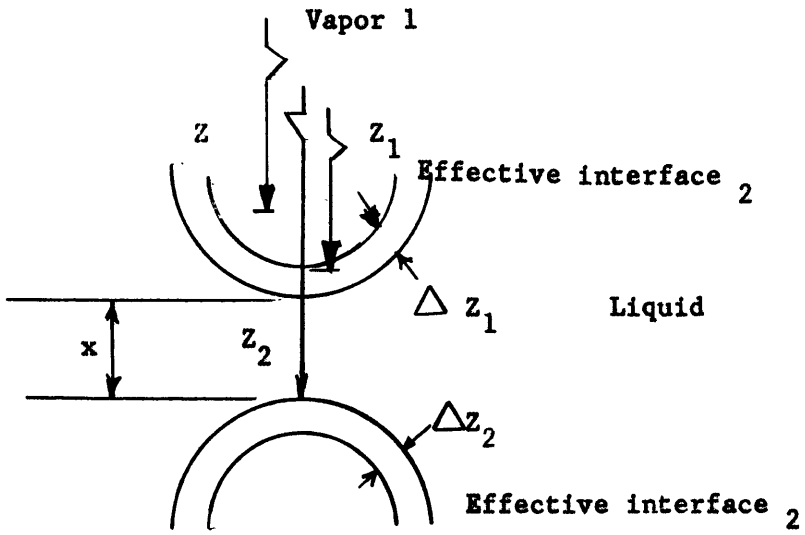

ΔZ_1 = the effective thickness of the vapor-liquid interface such that the substance in coordinates $Z_1 - \delta < Z < Z_1$ and the substance in coordinates $Z_1 + \Delta Z_1 < Z < Z_1 + \Delta Z_1 + \delta$ can be respectively replaced by bulk vapor in bubble 1 and bulk liquid of the surroundings without changing any characteristic of the interface, and such that the substances in the coordinates $Z_1 < Z < Z_1 + \delta$ and the substances in the coordinates $Z_1 + \Delta Z_1 - \delta < Z < Z_1 + Z_1$ cannot be replaced respectively by bulk vapor in bubble 1 and bulk liquid of the surroundings without changing any characteristic of the interface.

ΔZ_2 = the effective vapor-liquid interface thickness of bubble 2.

Z_1 = inside coordinate of the effective interface in film 1.

Z_2 = outside coordinate of the effective interface in film 2.

$x \equiv Z_2 - Z_1 + \Delta Z_1$ separation distance

Z = a datum variable

FIGURE 16

BUBBLE COALESCENCE MODEL

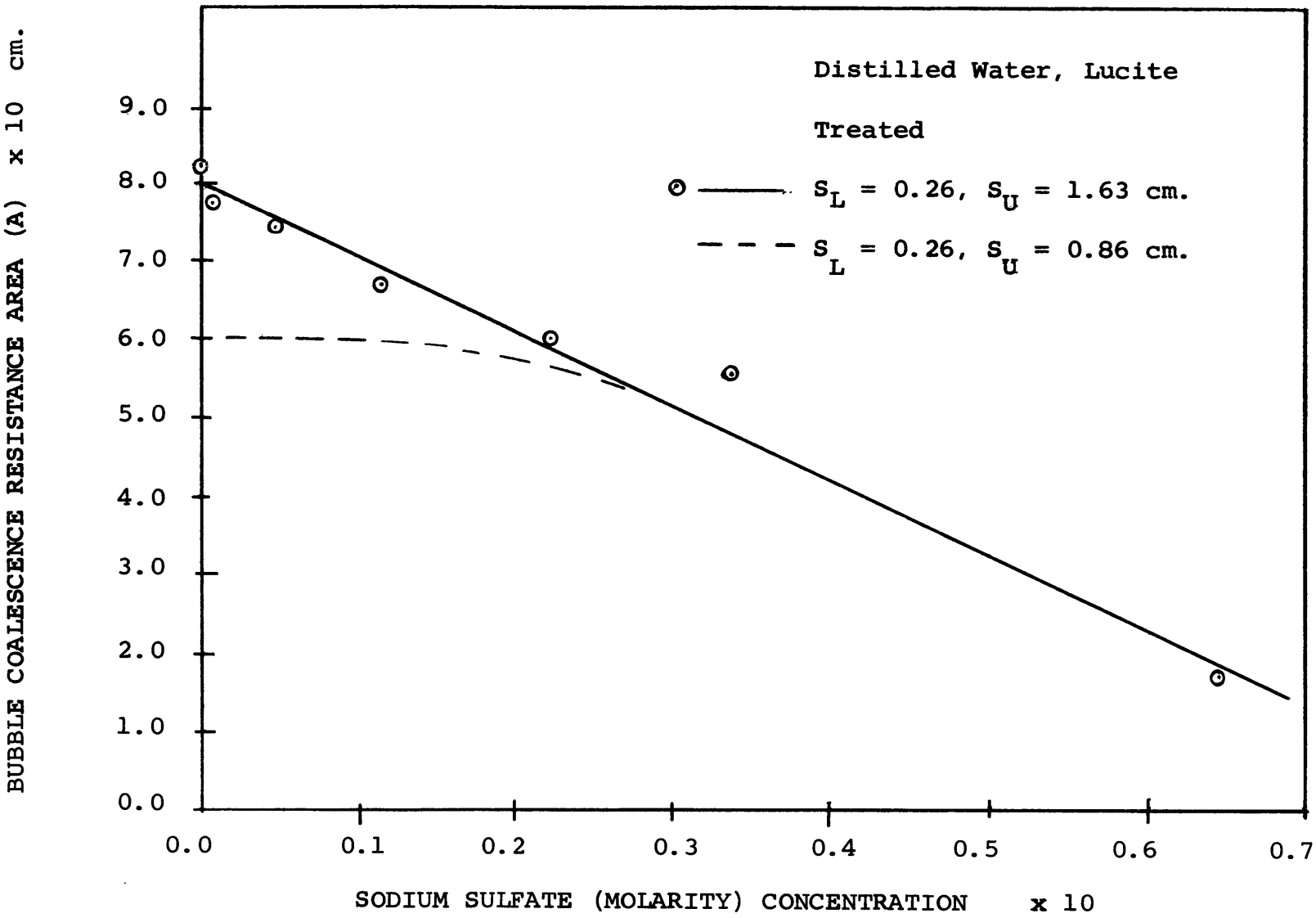
BUBBLE COALESCENCE RESISTANCE AREA (A) x 10 cm.
9.0
8.0
7.0
6.0
5.0
4.0
3.0
2.0
1.0
0.0
0.0
0.1
0.2
0.3
0.4
0.5
0.6
0.7
SODIUM SULFATE (MOLARITY) CONCENTRATION x 10
Distilled Water, Lucite
Treated
S_L = 0.26, S_U = 1.63 cm.
S_L = 0.26, S_U = 0.86 cm.

FIGURE 17

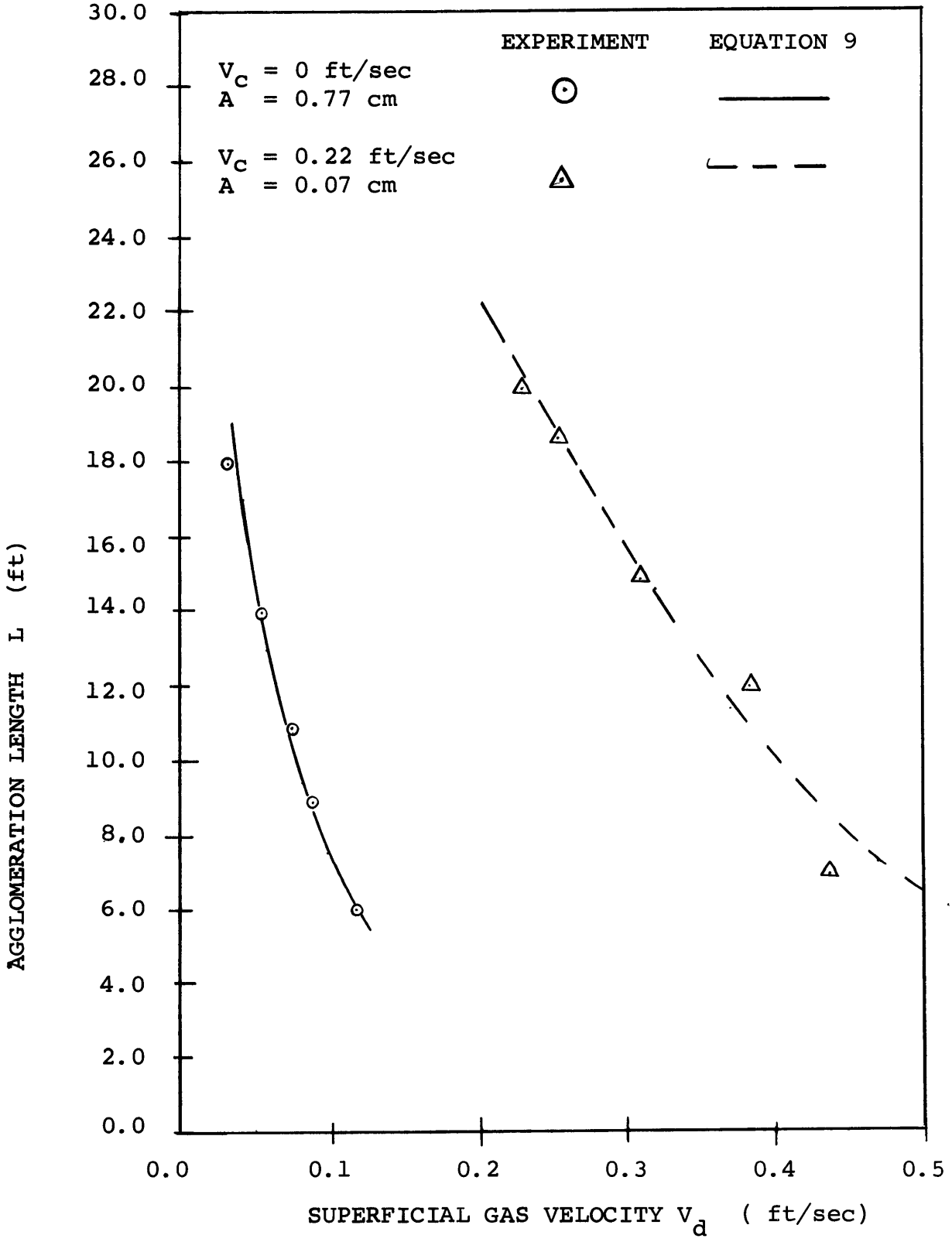

COMPARISON OF EXPONENTIAL CORRELATION EQUATION WITH EXPERIMENT

FIGURE 18

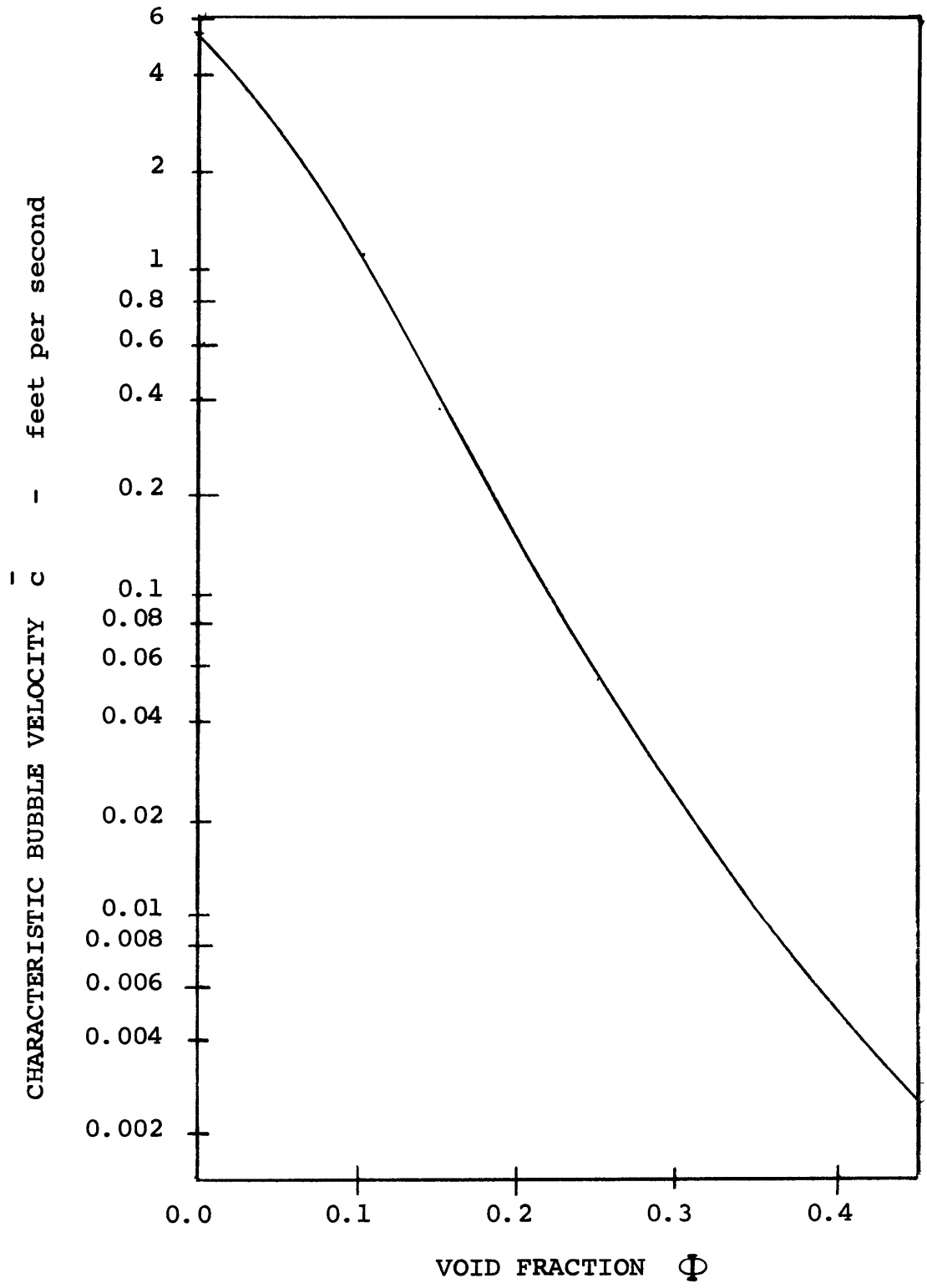

CHARACTERISTIC BUBBLE VELOCITY VERSUS VOID FRACTION

FIGURE 19

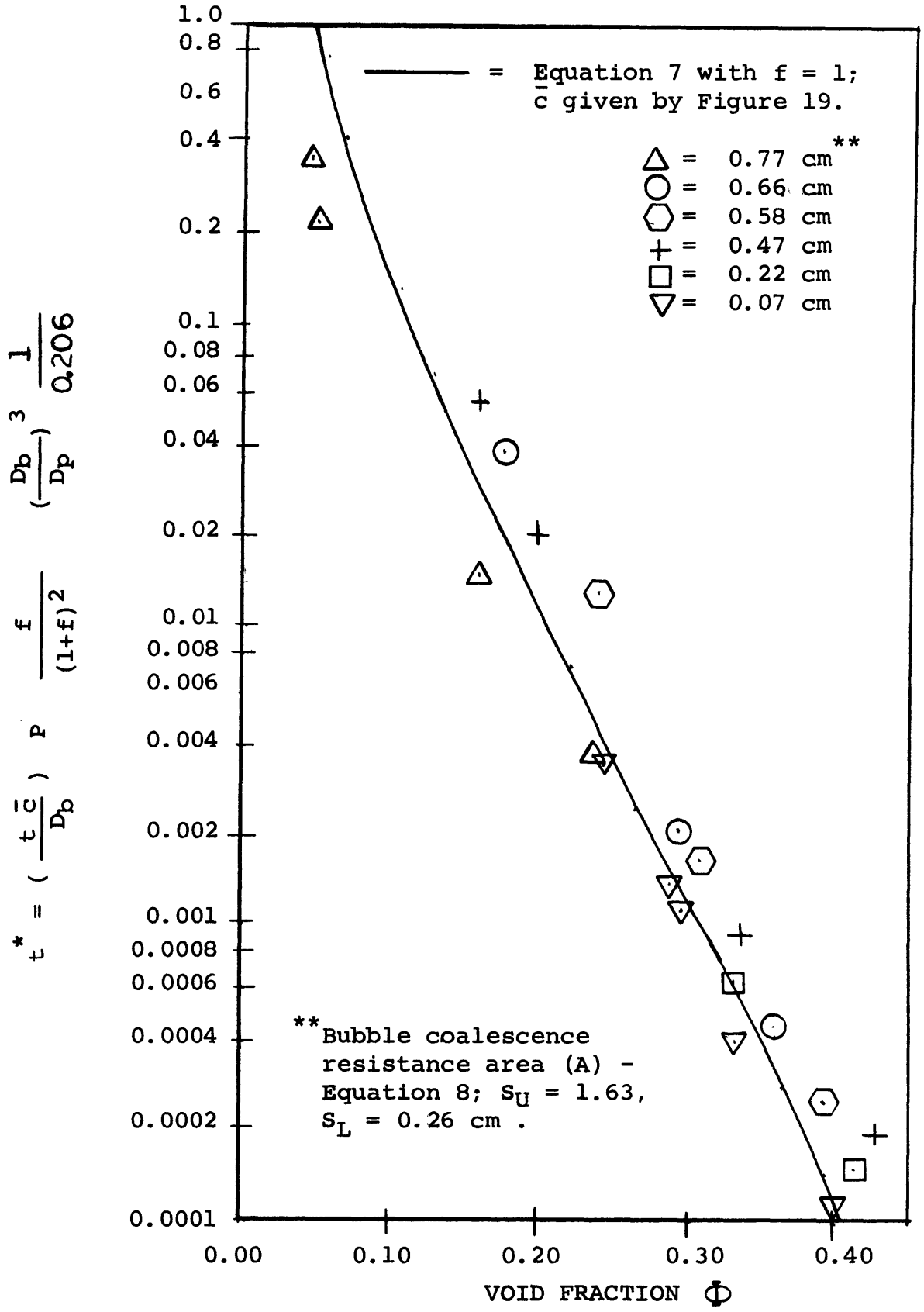

COMPARISON OF COLLISION MODEL THEORY WITH EXPERIMENTS

FIGURE 20

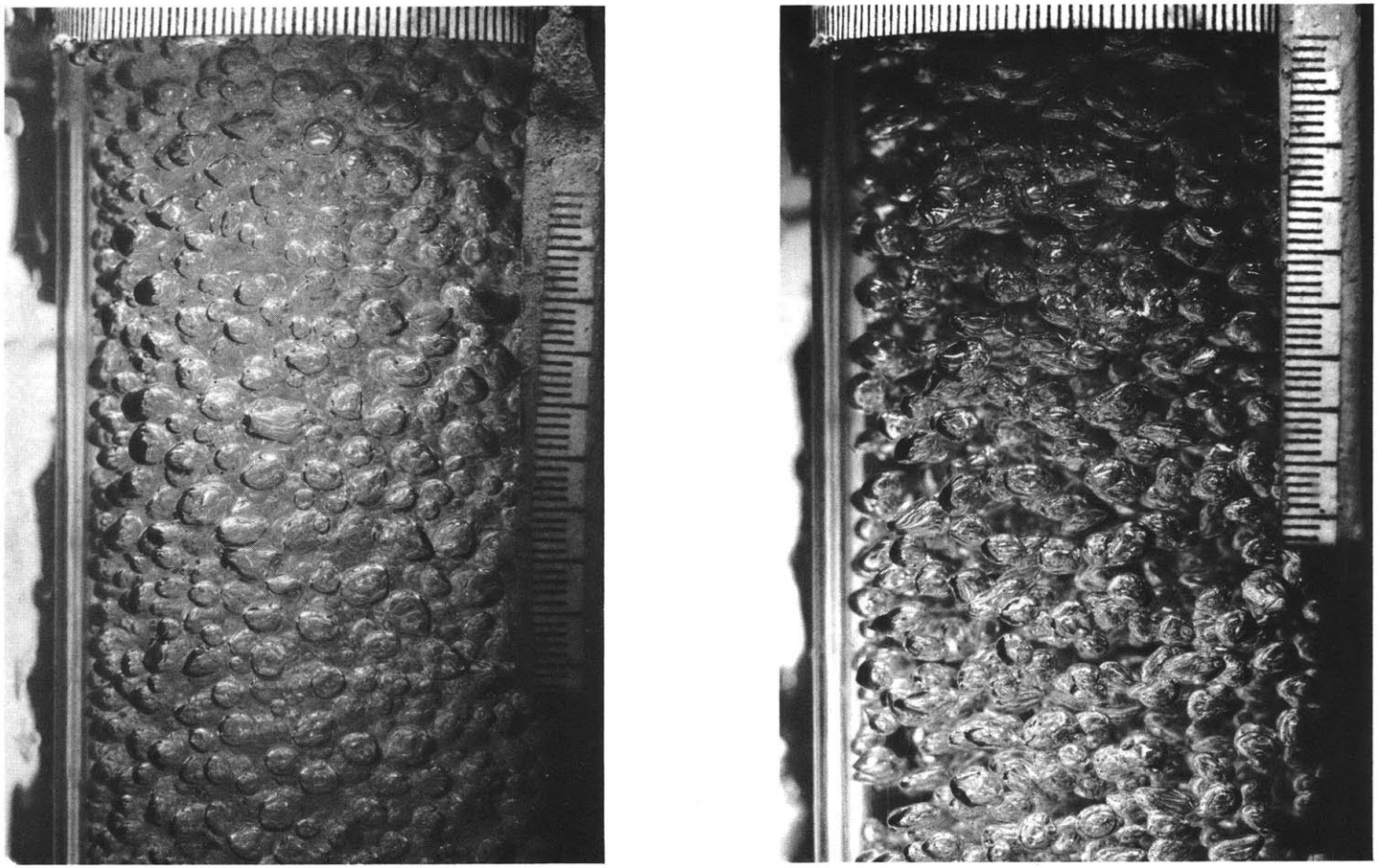

(a) (b)

BUBBLES AT CO-CURRENT APPARATUS

TUBE INLET

FIGURE 21

APPENDIX III

G. B. WALLIS - VOLUME VOID FRACTION EQUATION (4)

Essentially, the equation presented by Wallis (4) is of the form:

$$\frac{V_d}{\Phi(1-\Phi)} - \frac{V_c}{(1-\Phi)} = V_{b\,\infty} \qquad (10)$$

where $V_{b\,\infty}$ is the terminal velocity of a bubble rising in an infinite medium (22). However, the equation is conspicuously independent of pipe diameter.

The experiment shows that in order to correlate data, must equal 0.66 ft/sec. It is highly probable that Equation (10) is correct in a infinite liquid medium. To correct for tube diameter, Equation (10) is rewritten as:

$$\frac{V_d}{\Phi(1-\Phi)} - \frac{V_c}{(1-\Phi)} = n_1 V_b = C_1 \qquad (11)$$

where n_1 is primarily dependent upon tube diameter.

For a bubble with a diameter equal to 0.15 inches, $V_{b\,\infty}$ equals 0.85 ft/sec. In order to determine whether or not this value of $V_{b\,\infty}$ is applicable to a two inch tube, a simple experiment was conducted in the following manner.

The tube in the co-current apparatus is filled with water to a height of 4 feet. Gas is then injected into the system and the height of the bubble mixture is noted. The necessary precautionary steps are taken to insure bubble flow. There is also some evidence that C_1 is dependent upon Φ, especially at high Φ values.

For low Φ values ($0 < \Phi < 0.20$) Equation (11) correlates all experimental data within $\pm$ 5%* with $C_1 = 0.66$. Some experiments were performed when $V_c \neq 0$. However, due to tube length, limited shut down speed, and separator tank drainage problems, the results only indicate that $C_1 = 0.66$ is probably correct.

---

* If $V_c = 0$